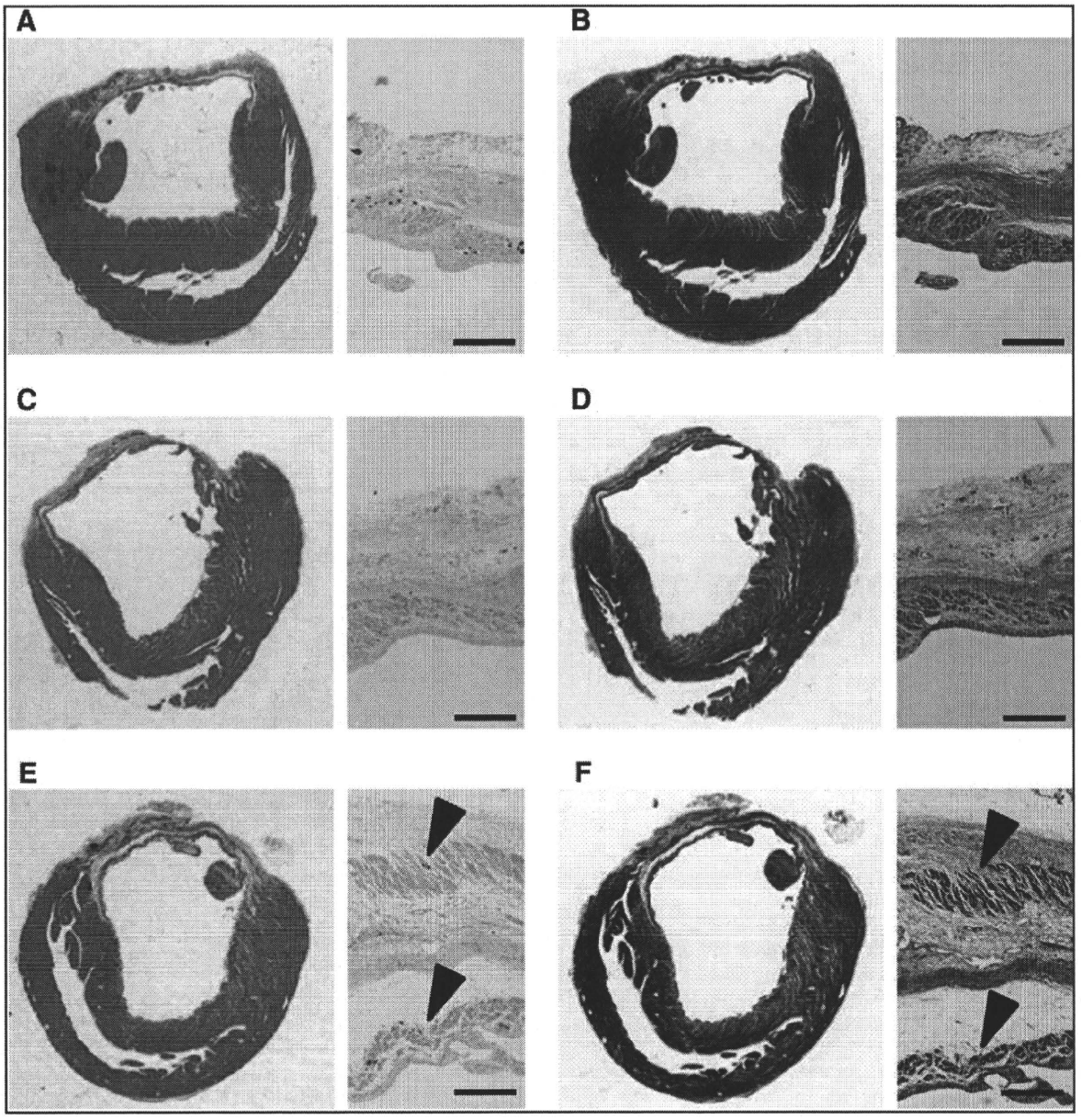

FIG. 3. Effects of CLC transplantation on cardiac structure. Photomicrographs showing representative myocardial sections stained with hematoxylin and eosin (**A, C, D**) and Masson trichrome (**B, D, F**) in the individual groups. The transplanted CLC patch reversed wall thinning of the infracted myocardium and another cardiac muscle was layered onto the transplanted area (arrowheads). (**A, B**) Sham-operated MI control group; (**C, D**) noncommitted hADMSC patch-transplanted group; and (**E, F**) hADMSC-derived CLC patch-transplanted group. Bars = 200 μm.

layer of α-CA-positive cells was apparent in the tissues from noncommitted hADMSC-transplanted rats (Fig. 4A, C), whereas the CLC patch-transplanted group showed two cardiac muscle layers positive for α-CA (Fig. 4E, arrow and arrowhead). There were no human troponin I-positive cells in the sham-operated MI control group (Fig. 4B), but some were observed in the noncommitted hADMSC patch-transplanted group (Fig. 4D). As shown in Figure 4F, large amounts of human troponin I-positive myocardium was observed in the CLC-transplanted animals (arrow) in addition to some human troponin I-negative but α-CA-positive myocardium in the internal myocardial layer (Fig. 4E, F, arrowhead). These results indicated that CLCs can efficiently differentiate into cardiomyocytes *in situ*.

Discussion

There are several advantages to hADMSC-derived CLC patch transplantation for regeneration therapy. First, the source of adipose-derived cells is easily and safely accessible and the cells can be obtained in large quantities, without serious ethical issues. Second, hADMSCs differentiate into CLCs by induction with DMSO, which is available in current good manufacturing practice grade. Third, hADMSC-derived

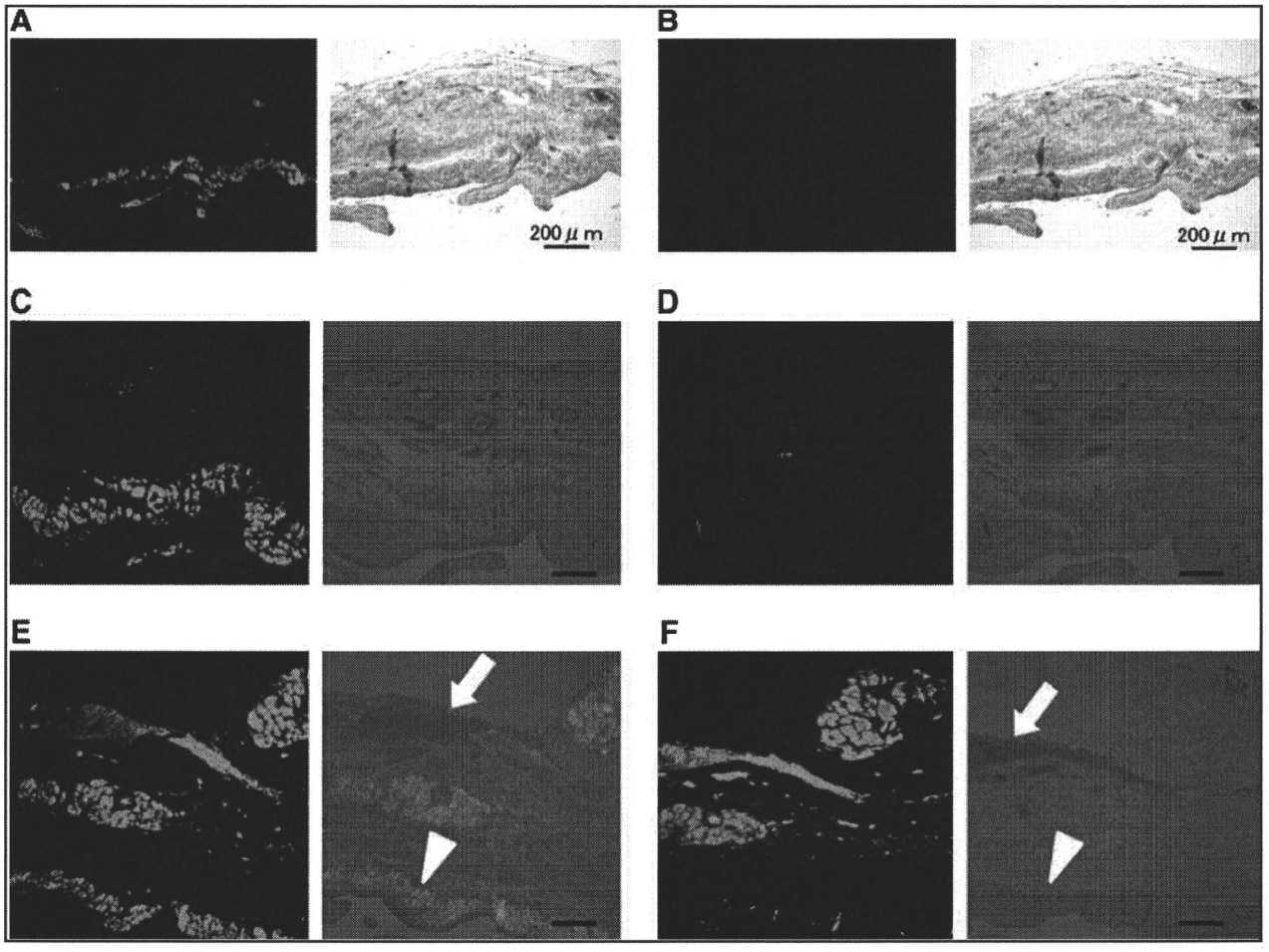

FIG. 4. CLCs differentiate into cardiac muscles *in situ*. Immunofluorescence with anti-α-CA (**A, C, E**) and anti-human-specific cardiac troponin I (**B, D, F**) antibodies, merged with phase contrast. In the hADMSC-derived CLC patch-transplanted groups, two cardiac muscle layers positive for α-CA are observed (**E**, arrow and arrowhead). A large mass of human troponin I-positive myocardium was observed in the CLC-transplanted tissues (**F**, arrows). In the same animals, the internal myocardium layer expressed α-CA but not human troponin I (**E, F**, arrowheads). (**A, B**) Sham-operated MI control group; (**C, D**) noncommitted hADMSC patch-transplanted group; and (**E, F**) CLC patch-transplanted group. Bars = 200 μm.

CLCs can differentiate into cardiomyocytes *in vivo* within the myocardial milieu, resulting in increment of myocardial muscle force. Finally, reconstruction of thick myocardial tissue rescued cardiac dysfunction after MI and improved long-term survival.

The choice of cell source is critical for realizing success in cellular therapy.[18] Liposuction surgeries yield from 100 mL to >3 L of lipoaspirate tissue.[19] The initial isolation of cells from adipose tissue was described by Bjorntorp *et al.*[14] This procedure was since modified to isolate cells from human adipose tissue specimens.[20–22] In this context, Zuk *et al.*[11] reported that the preadipocytes exhibited stem cell features as MSCs, currently known as ADMSCs. Because of the above-stated advantages of procuring cells for therapy from adipose tissues, hADMSCs present a potential and promising source for cellular therapy, even in patients with post-MI severe heart failure.

The *in vitro* differentiation of ADMSCs is now well reported, and experimental findings in recent years suggested considerable therapeutic potential for cellular replacement in the context of acute MI and chronic progressive cardiac disease.[23–27] Stem cells are differentiated into a cardiomyocyte lineage by treatment with 5-azacytidie, retinoic acid, oxytocin, and many other reagents.[28–32] We proposed that DMSO could differentiate hADMSCs into CLCs, based on the differentiation of P19 embryonic stems cells into cardiomyocytes with DMSO.[31–33] It was notable that DMSO is also available in current good manufacturing practice grade. Unfortunately, DMSO-treated hADMSCs did not show spontaneous beating as their terminal differentiation function, but the cells did express the mature markers α-*CA*, *myosin light chain*, and *myosin heavy chain* to a lesser extent. There are no reports of the use of DMSO to commit ADMSCs to a cardiomyocytic lineage. The mechanism by which DMSO elicits its effect on differentiation remains unclear. It is possible that DMSO increases intracellular calcium ion concentration, thereby elevating phosphatidylethanolamine levels in the cells and controlling the distribution of protein kinase C to commit the P19 stem cells.[33–36] These mechanisms should be investigated further in the near future.

The *in vitro* differentiation of ADMSCs has been well reported,[23–27] although only a few reports relate to the differentiation of these cells into cardiomyocytes *in vivo*. Recently,

Miyahara *et al.*[13] reported the use of monolayered ADMSCs for myocardial repair. In their study, rat ADMSCs were isolated and grown as intact monolayer sheets using temperature-responsive culture dishes. Placement of the ADMSC sheets onto a scarred myocardium in rats resulted in diminished scarring and enhanced cardiac structure and function. Histological analysis demonstrated that the engrafted ADMSC sheets grew to form a thickened layer over the infarcted muscle that included newly formed vessels and a few cardiomyocytes. In our study, hADMSC-derived CLCs differentiated into cardiomyocytes in a myocardial milieu, indicated by the immunohistological results in which transplanted cells expressed human troponin I *in vivo*. Newly developed myocardium might augment cardiac function, and thus hADMSC patch transplantation was performed as a control. Cardiac dysfunction was rescued in a short term, although the numbers of cardiomyocytes derived from transplanted cells were low. In this context, Gimble *et al.*[19] suggested that hADMSCs might secrete angiogenic factors and/or antiapoptotic factors.

Transplantation of the hADMSC-derived CLC regenerated the thick myocardial tissues, rescued cardiac dysfunction after MI, and improved long-term survival rate compared with the noncommitted hADMSCs and sham-operated MI controls. The existing literature suggests that ADMSCs can be engrafted and survive within an infarcted myocardial milieu, acquire phenotypic markers consistent with cardiomyocytic and vascular-related lineages, and have a positive impact on structural and functional endpoints.[19,23–27] These are desirable outcomes for cardiac function and survival. However, few reports have applied long-term observation of the transplanted animals. Our study therefore observed the three rat groups for 16 weeks after transplantation. Only CLC transplantation provided the desired outcome at the experimental endpoint. Despite these encouraging results, much progress is needed to realize the hope of cell therapies for myocardial damage. First, delivery of the cell sheets to patients should be optimized for each given disease. Second, the issue of vascularization should be considered in the infracted or affected tissues after transplantation, because many small CLC patches would be necessary for a clinical cure. Finally, the value and impact of CLC patch transplantation should be confirmed in large animal models before embarking on clinical applications.

In conclusion, we showed that the phenotype of hADMSCs could be changed to that of CLCs by induction with DMSO. These hADMSC-derived CLCs engrafted into a scarred myocardium and differentiated into cardiomyocytes. The CLC patch transplantation also resulted in recovery of cardiac function and improved survival rate. Thus, transplantation of hADMSC-derived CLC patches in heart patients might be a potentially effective therapeutic strategy for cardiac tissue regeneration in the near future.

Acknowledgments

This report was supported in part by a grant-in-aid for Yoshiki Sawa from the New Energy and Industrial Technology Development Organization of Japan and in part by a grant-in-aid for Akifumi Matsuyama from the Ministry of Education, Culture, Sports, Science, and Technology of Japan.

Disclosure Statement

No competing financial interests exist.

References

1. Miyagawa, S., Sawa, Y., Taketani, S., Kawaguchi, N., Nakamura, T., Matsuura, N., and Matsuda, H. Myocardial regeneration therapy for heart failure hepatocyte growth factor enhances the effect of cellular cardiomyoplasty. Circulation **105,** 2556, 2002.
2. Miyagawa, S., Matsumiya, G., Funatsu, T., Yoshitatsu, M., Sekiya, N., Fukui, S., Hoashi, T., Hori, M., Yoshikawa, H., Kanakura, Y., Ishikawa, J., Aozasa, K., Kawaguchi, N., Matsuura, N., Myoui, A., Matsuyama, A., Ezoe, S., Iida, H., Matsuda, H., and Sawa, Y. Combined autologous cellular cardiomyoplasty using skeletal myoblasts and bone marrow cells for human ischemic cardiomyopathy with left ventricular assist system implantation: report of a case. Surg Today **39,** 133, 2009.
3. Taylor, D.A. Cell-based myocardial repair: how should we proceed? Int J Cardiol **95,** S8, 2004.
4. Chachques, J.C., Acar, C., Herreros, J., Trainini, J.C., Prosper, F., D'Attellis, N., Fabiani, J.N., and Carpentier, A.F. Cellular cardiomyoplasty: clinical application. Ann Thorac Surg **77,** 1121, 2004.
5. Pallante, B.A., and Edelberg, J.M. Cell sources for cardiac regeneration—which cells and why. Am Heart Hosp J **4,** 95, 2006.
6. Chiu, R.C. MSC immune tolerance in cellular cardiomyoplasty. Semin Thorac Cardiovasc Surg **20,** 115, 2008.
7. Pittenger, M.F., Mackay, A.M., Beck, S.C., Jaiswal, R.K., Douglas, R., Mosca, J.D., Moorman, M.A., Simonetti, D.W., Craig, S., Marshak, D.R. Multilineage potential of adult human mesenchymal stem cells. Science **284,** 143, 1999.
8. Jiang, Y., Jahagirdar, B.N., Reinhardt, R.L., Schwartz, R.E., Keene, C.D., Ortiz-Gonzalez, X.R., Reyes, M., Lenrik, T., Lund, T., Blackstad, M., Du, J., Aldrich, S., Lisberg, A., Low, W.C., Largaespada, D.A., Vertaille, C.M. Pluripotency of mesenchymal stem cells derived from adult marrow. Nature **418,** 41, 2002.
9. Pittenger, M.F., and Martin, B.J. Mesenchymal stem cells and their potential as cardiac therapeutics. Circ Res **95,** 9, 2004.
10. Toma, C., Pittenger, M.F., Cahill, K.S., Byrne, B.J., and Kessler, P.D. Human mesenchymal stem cells differentiate to a cardiomyocyte phenotype in the adult murine heart. Circulation **105,** 93, 2002.
11. Zuk, P.A., Zhu, M., Mizuno, H., Huang, J., Futrell, J.W., Katz, A.J., Benhaim, P., Lorenz, H.P., and Hedrick, M.H. Multilineage cells from human adipose tissue: implications for cell-based therapies. Tissue Eng **7,** 211, 2001.
12. Katz, A.J., Tholpady, A., Tholpady, S.S., Shang, H., and Ogle, R.C. Cell surface and transcriptional characterization of human adipose-derived adherent stromal (hADAS) cells. Stem Cells **23,** 412, 2005.
13. Miyahara, Y., Nagaya, N., Kataoka, M., Yanagawa, B., Tanaka, K., Hao, H., Ishino, K., Ishida, H., Shimizu, T., Kangawa, K., Sano, S., Okano, T., Kitamura, S., and Mori, H. Monolayered mesenchymal stem cells repair scarred myocardium after myocardial infarction. Nat Med **12,** 459, 2006.
14. Bjorntorp, P., Karlsson, M., Pertoft, H., Pettersson, P., Sjostrom, L., and Smith, U. Isolation and characterization of cells from rat adipose tissue developing into adipocytes. J Lipid Res **19,** 316, 1978.

15. Memon, I.A., Sawa, Y., Fukushima, N., Matsumiya, G., Miyagawa, S., Taketani, S., Sakakida, S.K., Kondoh, H., Aleshin, A.N., Shimizu, T., Okano, T., and Matsuda, H. Combined autologous cellular cardiomyoplasty with skeletal myoblasts and bone marrow cells in canine hearts for ischemic cardiomyopathy. J Thorac Cardiovasc Surg **130,** 1333, 2005.
16. Miyagawa, S., Sawa, Y., Sakakida, S., Taketani, S., Kondoh, H., Memon, I.A., Imanishi, Y., Shimizu, T., Okano, T., and Matsuda, H. Tissue cardiomyoplasty using bioengineered contractile cardiomyocyte sheets to repair damaged myocardium: their integration with recipient myocardium. Transplantation **80,** 1586, 2005.
17. Hata, H., Matsumiya, G., Miyagawa, S., Kondoh, H., Kawaguchi, N., Matsuura, N., Shimizu, T., Okano, T., Matsuda, H., and Sawa, Y. Grafted skeletal myoblast sheets attenuate myocardial remodeling in pacing-induced canine heart failure model. J Thorac Cardiovasc Surg **132,** 918, 2006.
18. Murry, C.E., Reinecke, H., and Pabon, L.M. Regeneration gaps: observations on stem cells and cardiac repair. J Am Coll Cardiol **47,** 1777, 2006.
19. Gimble, J.M., Katz, A.J., and Bunnel, B.A. Adipose = derived stem cells for regenerative medicine. Circ Res **100,** 1249, 2007.
20. Deslex, S., Negrel, R., Vannier, C., Etienne, J., and Ailhaud, G. Differentiation of human adipocyte precursors in a chemically defined serum-free medium. Int J Obes **11,** 19, 1987.
21. Hauner, H., Entenmann, G., Wabitsch, M., Gaillard, D., Ailhaud, G., Negrel, R., and Pfeiffer, E.F. Promoting effect of glucocorticoids on the differentiation of human adipocyte precursor cells cultured in a chemically defined medium. J Clin Invest **84,** 1663, 1989.
22. Hauner, H., Wabitsch, M., and Pfeiffer, E.F. Differentiation of adipocyte precursor cells from obese and nonobese adult women and from different adipose tissue sites. Horm Metab Res Suppl **19,** 35, 1988.
23. Parker, A.M., and Katz, A.J. Adipose-derived stem cells for the regeneration of damaged tissues. Expert Opin Biol Ther **6,** 567, 2006.
24. Rangappa, S., Entwistle, J.W., Wechsler, A.S., and Kresh, J.Y. Cardiomyocyte-mediated contact programs human mesenchymal stem cells to express cardiogenic phenotype. J Thorac Cardiovasc Surg **126,** 124, 2003.
25. Gaustad, K.G., Boquest, A.C., Anderson, B.E., Gerdes, A.M., and Collas, P. Differentiation of human adipose tissue stem cells using extracts of rat cardiomyocytes. Biochem Biophys Res Commun **314,** 420, 2004.
26. Planat-Benard, V., Menard, C., Andre, M., Puceat, M., Perez, A., Garcia-Verdugo, J.M., Penicaud, L., and Casteilla, L. Spontaneous cardiomyocyte differentiation from adipose tissue stroma cells. Circ Res **94,** 223, 2004.
27. Strem, B.M., Zhu, M., Alfonso, Z., Daniels, E.J., Schreiber, R., Beygui, R., MacLellan, W.R., Hedrick, M.H., and Fraser, J.K. Expression of cardiomyocytic markers on adipose tissue-derived cells in a murine model of acute myocardial injury. Cytotherapy **7,** 282, 2005.
28. Balana, B., Nicoletti, C., Zahanich, I., Graf, E.M., Christ, T., Boxberger, S., and Ravens, U. 5-Azacytidine induces changes in electrophysiological properties of human mesenchymal stem cells. Cell Res **16,** 949, 2006.
29. Gassanov, N., Er, F., Zagidullin, N., Jankowski, M., Gutkowska, J., and Hoppe, U.C. Retinoid acid-induced effects on atrial and pacemaker cell differentiation and expression of cardiac ion channels. Differentiation **76,** 971, 2008.
30. Paquin, J., Danalache, B.A., Jankowski, M., McCann, S.M., and Gutkowska, J. Oxytocin induces differentiation of P19 embryonic stem cells to cardiomyocytes. Proc Natl Acad Sci USA **99,** 9550, 2002.
31. Fathi, F., Murasawa, S., Hasegawa, S., Asahara, T., Kermani, A.J., and Mowla, S.J. Cardiac differentiation of P19CL6 cells by oxytocin. Int J Cardiol **134,** 75, 2009.
32. Swijnenburg, R.J., van der Bogt, K.E., Sheikh, A.Y., Cao, F., and Wu, J.C. Clinical hurdles for the transplantation of cardiomyocytes derived from human embryonic stem cells: role of molecular imaging. Curr Opin Biotechnol **18,** 38, 2007.
33. Skerjanc, I.S. Cardiac and skeletal muscle development in P19 embryonal carcinoma cells. Trends Cardiovasc Med **9,** 139, 1999.
34. Xu, F.Y., Fandrich, R.R., Nemer, M., Kardami, E., and Hatch, G.M. The subcellular distribution of protein kinase C-alpha, -epsilon, and -zeta isoforms during cardiac cell differentiation. Arch Biochem Biophys **367,** 17, 1999.
35. Xu, F.Y., Kardami, E., Nemer, M., Choy, P.C., and Hatch, G.M. Elevation in phosphatidylethanolamine is an early but not essential event for cardiac cell differentiation. Exp Cell Res **256,** 358, 2000.
36. Monzen, K., Shiojima, I., Hiroi, Y., Kudoh, S., Oka, T., Takimoto, E., Hayashi, D., Hosoda, T., Habara-Ohkubo, A., Nakaoka, T., Fujita, T., Yazaki, Y., and Komuro, I. Bone morphogenetic proteins induce cardiomyocyte differentiation through the mitogen-activated protein kinase kinase kinase TAK1 and cardiac transcription factors Csx/Nkx-2.5 and GATA-4. Mol Cell Biol **19,** 7096, 1999.

Address correspondence to:
Akifumi Matsuyama, M.D., Ph.D.
Department of Somatic Stem Cell Therapy
Foundation for Biomedical Research and Innovation
1-5-4-305 Minatojima-minamimachi
Chuo-ku, Kobe 650-0047
Japan

E-mail: akifumi-matsuyama@umin.ac.jp

Received: June 1, 2009
Accepted: July 21, 2009
Online Publication Date: September 5, 2009

Cell Transplantation, Vol. 19, pp. 573–588, 2010

0963-6897/10 $90.00 + .00
DOI: 10.3727/096368909X486048
E-ISSN 1555-3892
www.cognizantcommunication.com

Bcl-2 Expression Enhances Myoblast Sheet Transplantation Therapy for Acute Myocardial Infarction

Katsukiyo Kitabayashi,*†‡[1] Antti Siltanen,†[1] Tommi Pätilä,†‡
Muhammad Ali Asim Mahar,† Ilkka Tikkanen,§ Jonna Koponen,¶
Masamichi Ono,* Yoshiki Sawa,* Esko Kankuri,†‡ and Ari Harjula†‡

*Department of Cardiovascular Surgery, Osaka University Graduate School of Medicine, Osaka, Japan
†Institute of Biomedicine, Pharmacology, University of Helsinki, Helsinki, Finland
‡Department of Cardiothoracic Surgery, Helsinki University Meilahti Hospital, Helsinki, Finland
§Minerva Foundation Institute for Medical Research, Helsinki, Finland
¶A.I. Virtanen Institute for Molecular Sciences, Department of Biotechnology and Molecular Medicine, University of Kuopio, Kuopio, Finland

Myoblast sheet transplantation is a promising novel treatment modality for heart failure after an ischemic insult. However, low supply of blood and nutrients may compromise sheet survival. The aim of this study was to investigate the effect of mitochondria-protective Bcl-2-modified myoblasts in cell sheet transplantation therapy. In the Bcl-2-expressing rat L6 myoblast sheets (L6-Bcl2), increased expression of myocyte markers and angiogenic mediators was evident compared to wild-type (L6-WT) sheets. The L6-Bcl2 sheets demonstrated significant resistance to apoptotic stimuli, and their differentiation capacity in vitro was increased. We evaluated the therapeutic effect of Bcl-2-modified myoblast sheets in a rat model of acute myocardial infarction (AMI). Sixty-four Wistar rats were divided into four groups. One group underwent AMI ($n = 22$), another AMI and L6-WT sheet transplantation ($n = 17$), and a third AMI and L6-Bcl2 sheet transplantation ($n = 20$). Five rats underwent a sham operation. Echocardiography was performed after 3, 10, and 28 days. Samples for histological analysis were collected at the end of the study. After AMI, the Bcl-2-expressing sheets survived longer on the infarcted myocardium, and significantly improved cardiac function. L6-Bcl2 sheet transplantation reduced myocardial fibrosis and increased vascular density in infarct and border areas. Moreover, the number of c-kit-positive and proliferating cells in the myocardium was increased in the L6-Bcl2 group. In conclusion, Bcl-2 prolongs survival of myoblast sheets, increases production of proangiogenic paracrine mediators, and enhances the therapeutic efficacy of cell sheet transplantation.

Key words: Apoptosis; Bcl-2; Cell sheet therapy; Myoblast; Myocardial infarction

INTRODUCTION

Although the first myoblast transplantation therapies were administered more than a decade ago for the treatment of heart failure (29,34), problems associated with cell injections, such as the massive loss of donor cells, inadequate cell proliferation in the host myocardium, and arrhythmogenicity, remain to be solved. To overcome some of these problems, epicardial transplantation of cell sheets provides a conceptual alternative and a minimally invasive method for cell delivery. In this system, a tissue-engineered multicellular patch or cell sheet is made with a temperature-responsive cell culture dish (22,31). With this technique freely transplantable cell sheets consisting of 3–6 million cells can easily be manufactured with no added scaffold material. Such sheets can then be implanted on top of the injured myocardium to which they adhere immediately. Moreover, therapy can be enhanced by piling two or more layers of sheets on top of each other. The superiority of sheet transplantation over intramyocardial injections for cell therapy of heart failure has been demonstrated in both small and large animal studies (12,15,20). The therapeutic effect of cell sheets is considered to be mediated via finite production of paracrine effectors that locally stimulate the underlying injured myocardium. In models of cardiac is-

Received August 28, 2009; final acceptance December 30, 2009. Online prepub date: January 20, 2010.
[1]These authors provided equal contribution.
Address correspondence to Antti Siltanen, Institute of Biomedicine, Pharmacology, Biomedicum, P.O. Box 63, FIN-00014 University of Helsinki, 00290 Helsinki, Finland. Tel: +358-9-191-25362; Fax: +358-9-191-25364; E-mail: antti.siltanen@helsinki.fi

chemia and infarction, myoblast sheet therapy has been shown to inhibit fibrosis and to stimulate angiogenesis (20).

These previous studies have shown that multiple myoblast sheets are required for ischemic heart failure therapy. The sheets on the injured myocardium are exposed to apoptotic stress and nutrient deprivation, and thus an increased number of cells are required for therapeutic benefit. In order to reduce the amount of transplanted sheets and to increase their tolerance of the death-promoting host environment, we investigated the effect of *bcl2* gene expression in myoblast sheets and their therapeutic efficacy in a rat model of acute myocardial infarction (AMI).

The family of Bcl-2 proteins comprises several members with anti- or proapoptotic functions. Bcl-2 itself is antiapoptotic, functioning in the mitochondrial pathway by counteracting functions of the proapoptotic Bax and Bak, and inhibiting cytochrome c release (26). Bcl-2 overexpression has been shown to promote cell survival and to inhibit cell death induced by such apoptosis-inducers as staurosporine, or by nutrient deprivation (6). Bcl-2 gene therapy has been used in cardiac cell therapy to prevent apoptosis upon cell injection into the myocardium (17,19).

In this study, we evaluated the Bcl-2 expression-mediated effects on L6 myoblast sheets both in vitro and in vivo. We first compared the apoptosis resistance and gene expression profiles of wild-type and Bcl-2-modified L6 myoblast monolayers and sheets. We then expanded these results to an in vivo setting, and evaluated the effects of wild-type and Bcl-2-overexpressing myoblast sheet transplantation in a rat model of AMI.

MATERIALS AND METHODS

Cell Culture and Sheets

The L6 rat skeletal myoblast cell line was obtained from the American Type Culture Collection (CRL-1458, Manassas, VA). Cells were cultured at 37°C with 5% CO_2 in growth medium (DMEM supplemented with 10% FCS and antibiotics), passaged three times weekly, and kept at 60% confluency to retain their differentiation potential. Passages 5 to 15 were used for the experiments. Cell sheets were formed by plating 6×10^6 myoblasts on thermoreactive culture dishes (CellSeed, Tokyo, Japan) to achieve sheet thickness of approximately five cell layers. Cells were incubated for 16 h at 37°C to induce sheet formation. The sheets detached spontaneously at room temperature within 45 min, and were then washed once with growth medium.

Measurement of Proliferation, Apoptosis, and Differentiation

Myoblast viability after 48-h serum deprivation or staurosporine treatment was assessed by the mitochondria-dependent reduction of 3-[4,5-dimethylthiazol-2-yl]-2,5-di-phenyltetrazolium bromide (MTT) to formazan (Roche, Mannheim, Germany) as described previously (33). Briefly, NADPH produced by the cells was visualized by adding MTT (10 µl, 5 mg/ml in PBS) to 100 µl of cell suspension. Following a 4-h incubation period at 37°C, the samples were dissolved in DMSO, and the amount of formazan dye generated was quantified (A540 nm/A650 nm). Cell adherence was determined 48 h after treatment. Nuclei were stained with DAPI, and cells were washed thoroughly with PBS. Cell nuclei were counted with CellC software version 1.11 (Selinummi and Seppälä, Tampere University of Technology, www.cs.tut.fi/sgn/csb/cellc). The early phase of apoptosis, characterized by phosphatidyl serine translocation, was determined 24 h after serum deprivation or staurosporine treatment by cell surface annexin V binding (Invitrogen, Carlsbad, CA). Fluorescence (340 nm/460 nm) was measured with Wallac Victor2 (Perkin-Elmer, Wellesley, MA). Myoblast sheet apoptosis was determined by measuring caspase-3 activity after the induction of apoptosis by either serum deprivation or staurosporine for 24 h. Caspase-3 activity was measured using EnzChek® caspase-3 assay kit (Invitrogen). For differentiation, sheets were deprived of serum to induce myoblast differentiation into myotubes. Western blotting samples were then collected for evaluation of troponin T and myogenin expression.

VEGF-A Measurements

VEGF-A protein secretion from myoblast sheets was determined from growth medium conditioned for 48 h using a rat VEGF DuoSet™ ELISA kit (R&D Systems, Minneapolis, MN) according to the manufacturer's instructions. VEGF-A expression was determined from staurosporine-treated or nutrient-deprived sheets.

Bcl-2 Overexpression and Transfection

pBabepuro-*bcl2* retroviral vector was a kind gift from Dr. Juha Klefström, University of Helsinki, Finland (14). L6 myoblasts were transfected with incubation for 48 h in the presence of retroviral vector and 8 µg/ml polybrene (Sigma-Aldrich, St. Louis, MO). Transfected cells were then selected with 2 µg/ml puromycin (Sigma) for 48 h.

Western Blotting

Western blotting samples were prepared in Laemmli sample buffer (Bio-Rad Laboratories, Redmond, WA). Detection was carried out as previously described (3) using appropriate alkaline phosphatase-conjugated secondary antibodies. The primary antibodies used were mouse monoclonal anti-Bcl-2 (610539, clone 7, BD Biosciences, San Jose, CA), mouse monoclonal anti-myogenin (sc-12732, clone F5D, Santa Cruz Biotechnology

Inc., Santa Cruz, CA), and mouse monoclonal anti-troponin T (T6277, clone JLT-12, Sigma-Aldrich).

Immunofluorescence Imaging

Cells were grown on coverslips for 48 h prior to fixation with 4% paraformaldehyde and permeabilization with 0.2% Triton X-100. Coverslips were incubated with anti-Bcl-2 antibody, washed with PBS, and incubated with an appropriate Alexa-Fluor fluorophore-conjugated (Invitrogen) secondary antibody. Nuclei were stained with DAPI, and coverslips were mounted on microscopy slides with Vectashield mounting medium (Vector Laboratories, Burlingame, CA). Samples were visualized with an Olympus IX70 microscope (Olympus Finland, Vantaa, Finland).

RNA Extraction and Microarray

Myoblast sheets were prepared as described. After a 40-h incubation period to enable three-dimensional culture-induced gene expression in vitro, total RNA was isolated using the Trizol reagent (Invitrogen) according to the manufacturer's instructions. Further purification was carried out with an RNeasy Mini Kit (Qiagen, Hilden, Germany). RNA quality was verified with an Agilent 2100 bioanalyzer (Agilent Technologies, Palo Alto, CA). Purified RNA was synthesized into double-stranded cDNA with a Superscript Double-stranded cDNA Synthesis Kit (Invitrogen). A Bioarray High Yield RNA Transcript Labeling Kit (Enzo LifeSciences, Faimingdale, NY) was then used to synthesize cRNA. cDNA and cRNA products were purified with a GeneChip Sample Cleanup Module (Affymetrix, Santa Clara, CA). cRNA products were then used for fragmentation reaction and hybridized into the Affymetrix Rat Genome 230 2.0 GeneChip Array. After 18 h, chips were washed and stained with a GeneChip Fluidics Station 400 (Affymetrix), followed by chip scanning with a GeneChip Scanner 3000 7G (Affymetrix). Data analysis was performed with GeneSpring GX software, version 7.3.1 (Agilent Technologies), normalized to the median 50 percentile, and presented as gene expression fold changes.

Animals

This study used 92 male Wistar rats (250–400 g) of which 64 rats survived surgery and follow-up. The rats were divided into four groups: Group 1—control, left anterior descending coronary artery (LAD) ligation (n = 22); group 2—LAD ligation and L6-WT sheet transplantation (n = 17); group 3—LAD ligation and L6-Bcl2 sheet transplantation (n = 20); and group 4—sham operation (n = 5). All rats were euthanized 28 days after ligation. Experimental procedures were conducted according to the US National Institutes of Health Guide for the Care and Use of Laboratory Animals, and were evaluated and approved by the ethical committee of the Hospital District of Helsinki and Uusimaa, Meilahti Hospital, Department of Surgery.

LAD Ligation and Cell Sheet Transplantation

AMI was induced by ligation of LAD as previously described (23). Briefly, animals were anesthetized subcutaneously using 0.05 mg/kg of medetomidine (Orion Pharma Inc., Turku, Finland) and 5 mg/kg IP ketamine (Parke-Davis, Barcelona, Spain). They were then intubated, and a respirator served to maintain ventilation during surgery. The heart was exteriorized through a left thoracotomy and pericardiotomy. LAD was ligated 3 mm from its origin. Immediately after LAD ligation, two circular myoblast sheets (total 1.2×10^7 cells), approximately 25 mm in diameter, were placed on the left ventricular anterior wall for each rat in groups 2 and 3. Group 2 received L6-WT sheets and group 3 received L6-Bcl2 sheets. After sheet transplantation, the heart was returned to its normal position and covered with pericardium to avoid adhesion to the lung and to the chest wall, and to prevent movement of the sheets. Throughout surgery, normal body temperature was maintained with a thermal plate. After surgery, anesthesia was antagonized with atipamezole hydrochloride (1.0 mg/kg, SC, Orion Pharma Inc.). Buprenorphine hydrocholoride (0.05 mg/kg, SC, Reckitt and Colman Ltd, Hull, UK) was administered for postoperative analgesia.

Echocardiography

All rats underwent echocardiography under anesthesia 3 (baseline), 10, and 28 days after surgery. The animals were sedated with 0.5 mg/kg medetomidine and placed on a thermal plate. Measurements were performed with a 7.5 MHz transducer (MyLab®25, Esaote SpA, Genoa, Italy). Anterior wall thickness, posterior wall thickness at diastolic (AWTd, PWTd) and systolic (AWTs, PWTs) phases, and left ventricular diameter at diastolic (Dd) and systolic (Ds) phases were measured in the short-axis right parasternal projection just below the mitral valves. Units are presented in millimeters. Dd and Ds were used to calculate fraction shortening (LVFS) and ejection fraction (LVEF) percentage: LVFS (%) = (Dd – Ds)/Dd, andLVEF (%) = $(Dd^3 - Ds^3)/Dd^3$.

Histology and Immunostaining

At 28 days after surgery, the rats were euthanized after echocardiography. The heart was then excised and cut into four equal transverse parts. Two middle parts (next apex and next basal) were fixed in 4% neutral-buffered formalin for 48 h. The samples were then embedded in paraffin, and were cut into 4-μm-thick sections for histology and immunostaining. Sirius Red stain served to analyze fibrosis. Immunostaining was performed using a Ventana Discovery Automate (Ventana Medical Systems Inc, Tuczon, AZ). To demonstrate vas-

cular density, endothelial cells were stained with antibody against von Willebrand Factor (vWF, RB-281, Labvision Inc., Fremont, CA). Cell proliferation was evaluated using anti-Ki67 antibody (RM-9106, Labvision Inc.), and apoptosis was detected with antibody specifically recognizing active cleaved caspase-3 (CST #9664, Cell Signaling Technology Inc., Danvers, MA). The stem cell antigen, c-kit, was detected with an anti-c-kit antibody (RA14132, Neuromics, Northfield, MN). Sections stained for Ki67 proliferation-associated antigen were double-stained for myocytes using anti-tropomyosin antibody (MS-1256, Labvision Inc.).

Analysis of Fibrosis

Fibrosis was evaluated from scanned images of Sirius Red-stained sections. Percentage of fibrosis was calculated as Sirius Red-stained area divided by whole section area as evaluated using Photoshop 7.0 (Adobe Inc, San Jose, CA).

Analysis of Vascular Density, Cell Proliferation, Apoptosis, and c-kit-Positive Cells

The vWF- and Ki67-immunostained sections were photographed with a microscope (100× magnification) from six fields (two from infarcted area, two from border area, two from remote area). Vascular density and proliferating cell number were calculated with ImageJ (National Institutes of Health, Bethesda, MD, http://rsb.info.nih.gov/ij). Briefly, RGB images were background subtracted and divided into Hue-Saturation-Brightness channels from which the Brightness channel was further analyzed by thresholding for the staining intensities of vWF or Ki67. All images were processed with the same parameters using a preprogrammed macro. Data were collected separately for infarcted, border and remote areas. Apoptotic cells were manually counted as the number of positive cells for cleaved caspase-3 from six fields per slide. From c-kit-stained sections, the c-kit-positive cells were counted manually from the entire section.

Analysis of Sheet Survival In Vivo

A substudy was designed to specifically evaluate sheet survival on top of the infracted area. Six rats were used. L6-WT and L6-Bcl2 myoblasts were labeled with green fluorescent protein (GFP) by incubation with a lentiviral vector carrying the *gfp* gene and 8 μg/ml polybrene for 24 h. The lentiviral vector was a kind gift from Professor Seppo Ylä-Herttuala (AIV Institute, Kuopio, Finland). AMI, myoblast cell sheet formation, and transplantation were done as described earlier. Animals, each receiving either L6-WT-GFP ($n = 6$) or L6-Bcl2-GFP ($n = 6$) sheets, were euthanized and hearts excised at 3 weeks after the surgery. Bright field and fluorescence images of the excised heart surface were acquired from the site of transplantation using the Leica MZ FLIII stereomicroscope (Leica Microsystems, Wetzlar, Germany). From these images, the intensity of GFP signal was assessed with the ImageJ software. Images were background subtracted and the fluorescence intensity was measured from green channels of the RGB images.

Statistical Analysis

Data are presented as mean ± SEM. Differences between groups were compared using the Student *t*-test. The Bonferroni posttest was applied for correction with multiple comparisons. Statistical analyses were performed with Graph Pad Prism 4.0 (GraphPad Software Inc., San Diego, CA).

RESULTS

Bcl-2 Overexpression and Function in Myoblasts and Myoblast Sheets

Bcl-2 expression was introduced to the L6 rat myoblast cell line with pBabepuro retroviral vector carrying the *bcl2* gene. Bcl-2 protein expression was verified with Western blotting (Fig. 1A), and was 28-fold higher in transfected cells than in wild-type cells. Immunofluorescence detection of Bcl-2 demonstrated a granular cytosolic pattern, suggesting a mitochondrial localization (Fig. 1B). The resistance to apoptosis of transfected myoblasts was evaluated with MTT assay. After serum deprivation, L6-Bcl-2 cells showed 33% higher viability than did L6-WT cells (0.371 ± 0.002 and 0.279 ± 0.004, $p < 0.001$); the baseline values before treatment were 0.420 ± 0.004 and 0.443 ± 0.006 for L6-WT and L6-Bcl2, respectively. After staurosporine treatment, L6-Bcl2 cells showed 2.4-fold higher viability than did L6-WT cells (0.244 ± 0.012 and 0.102 ± 0.006, $p < 0.001$) (Fig. 1C); the baseline values were 0.481 ± 0.010 and 0.469 ± 0.015.

After 48-h serum deprivation or staurosporine treatment the number of adherent L6-Bcl2 cells was 2-fold and 1.6-fold higher than that of L6-WT cells, respectively ($p < 0.001$ for both treatments) (Fig. 1D). Overexpression of Bcl-2 also prevented the induction of apoptosis after serum deprivation or staurosporine treatment ($p < 0.001$ each) as detected by the binding of annexin V to cell surface phosphatidyl serine, an early marker for cellular apoptosis (Fig. 1E).

Both cell types efficiently formed cell sheets, and the introduced overexpression of Bcl-2 was retained. Both types of sheets showed similar proliferative activity as evaluated by Ki67 expression. L6-Bcl2 sheets showed fewer cells positive for active cleaved caspase-3 (Fig. 2A).

To study the functionality of Bcl-2, we measured the activity of caspase-3 in unstimulated, serum-deprived, or staurosporine-treated myoblast sheets after 24 h. We

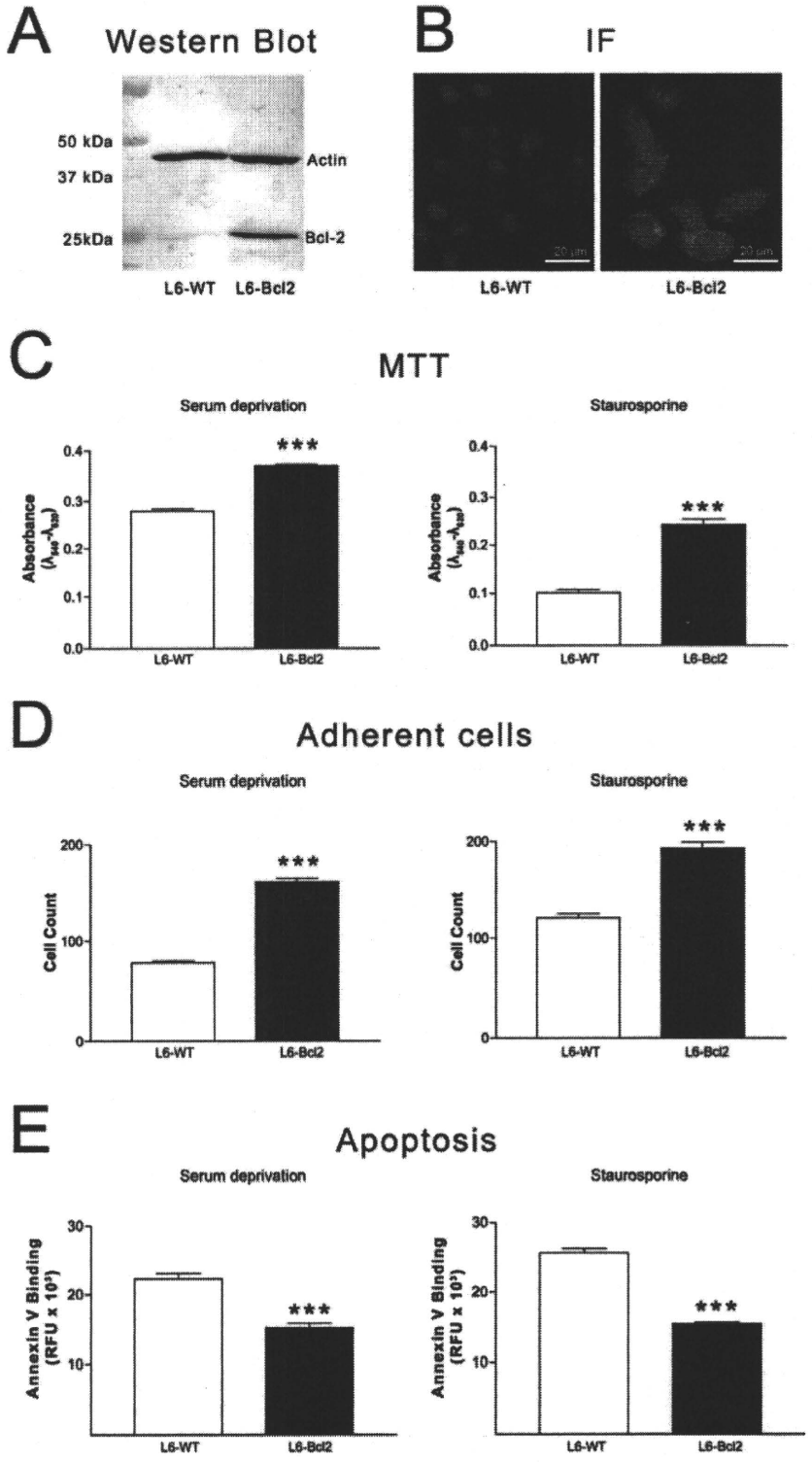

Figure 1. Expressional and functional characterization of Bcl-2 in L6 myoblasts. (A) Expression of Bcl-2 protein in wild-type (L6-WT) and Bcl-2-overexpressing (L6-Bcl2) myoblasts. (B) Immunofluorescence (IF) detection of Bcl-2 in L6 myoblasts, suggesting cytoplasmic and perinuclear localization. (C) Mitochondrial activity as measured with MTT assay in L6-WT and L6-Bcl2 in myoblast cultures treated for 48 h. (D) Number of adherent L6-WT and L6-Bcl2 myoblasts in cultures treated for 48 h. (E) Quantification of early apoptosis as measured by FITC-labeled annexin V binding to cell surface-translocated phosphatidyl serine. (C–E) Cultures deprived of serum (left panels), and cultures with apoptosis induced by staurosporine (80 ng/ml) (right panels).

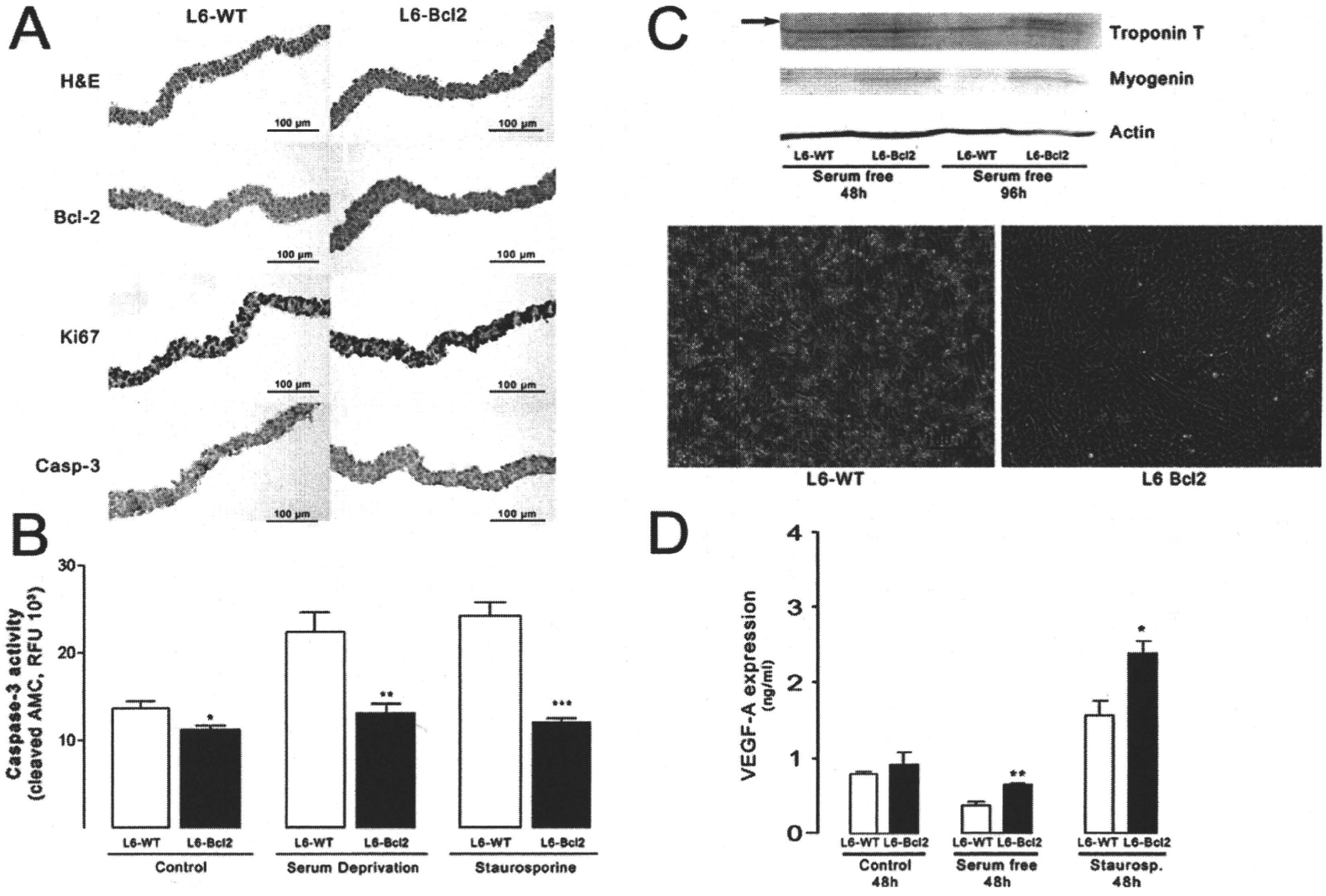

Figure 2. Immunohistochemistry, differentiation, and VEGF expression of wild type (L6-WT) and Bcl-2-overexpressing (L6-Bcl2) myoblast sheets. (A) Hematoxylin and eosin (H&E) stain, expression of Bcl-2 protein, cell proliferation as detected by the expression of proliferation-associated Ki67 antigen and the evaluation of apoptotic cells by immunodetection for active cleaved caspase-3. (B) Activation of caspase-3 in L6-WT and L6-Bcl2 myoblast sheets after 24 h in control, serum-deprived, and staurosporine-treated (10 ng/ml) sheets. (C) Immunoblots of myogenic differentiation markers troponin T and myogenin from L6-WT and L6-Bcl2 sheets after differentiation in serum-free medium for 96 h. Lower panels show phase contrast images demonstrating the formation of myotubes in L6-Bcl2 sheets. Cell detachment and death prevail in L6-WT sheets. (D) Amount of VEGF-A in culture medium of untreated, serum-deprived, and staurosporine-treated L6-WT and L6-Bcl2 sheets as determined with ELISA.

found that the introduction of Bcl-2 to myoblast sheets prevented the activation of effector caspase-3, whereas prolonged culture ($p = 0.041$) and cellular stress induced by serum deprivation ($p = 0.0097$) and staurosporine ($p = 0.0003$) led to caspase-3 activation in L6-WT sheets (Fig. 2B).

Because culture in reduced serum medium is standard practice for inducing differentiation of myoblasts (21), we used this method to investigate the differentiation of myoblast sheets. L6-Bcl2 myoblasts differentiated into myotubes as evaluated by the expression of differentiation markers troponin T and myogenin, whereas L6-WT myoblasts underwent cell death instead of differentiation under serum starvation. After prolonged culture, L6-WT sheets showed signs of disruption whereas cell survival in L6-Bcl2 sheets was predominant, and myotubes were visible (Fig. 2C).

Bcl-2 Induces Expression of Proangiogenic Mediators in Myoblast Sheets

Because Bcl-2 expression has been shown to affect several cellular processes (5), we used whole-genome microarrays to investigate the effect of *bcl2* gene transduction on gene expression in myoblasts. Interestingly, in monolayer cultures no differences in gene expression, other than increased *bcl2*, were observed between L6-WT and L6-Bcl2 cells (data not shown). When myoblast sheets were formed, however, distinct differences emerged (Table 1). Interestingly, the most striking induction emerged in genethonin, thus suggesting a specific increase in muscle-related gene expression (4). Of significance to myoblast sheet transplantation and its paracrine effect, we observed induction in angiogenesis-associated genes, such as *vegf* and *plgf*, suggesting that the proangiogenic potential of myoblast sheet therapy is incremented by Bcl-2 (Table 1). For verification of the microarray results, we evaluated the production of VEGF from myoblast sheets. L6-Bcl2 sheets produced greater amounts of VEGF in the culture medium under serum deprivation ($p = 0.0014$) or staurosporine-induced stress ($p = 0.0383$) than did L6-WT sheets during the 48-h incubation period (Fig. 2D).

Bcl-2-Expressing Myoblast Sheets Enhance Ventricular Function After AMI

To study the increased therapeutic efficacy with L6-Bcl2 versus L6-WT sheet transplantation, we used the rat LAD ligation model. Table 2 shows cardiac performance data assessed with echocardiography at 3, 10, and 28 days after ligation and sheet transplantation.

The function of the left ventricle, as measured by LVEF and LVFS, improved only in the L6-Bcl2 sheet-treated group. These parameters were significantly enhanced at day 10, and remained elevated until the end of the study at day 28. At day 10, the LVEF of both the L6-WT and L6-Bcl2 groups recovered from baseline, whereas the LVEF of the control group decreased (L6-WT: $30.3 \pm 2.3\%$ to $32.2 \pm 2.1\%$, L6-Bcl2 $31.4 \pm 2.3\%$ to $37.80 \pm 1.9\%$, control: $32.6 \pm 1.7\%$ to $29.1 \pm 2.0\%$). Even at day 28, LVEF remained significantly higher in the L6-Bcl2 group than in the L6-WT and control groups (L6 Bcl2: $33.2 \pm 2.0\%$, vs. control: $27.3 \pm 2.2\%$, $p = 0.035$, and L6-WT: $29.1 \pm 1.4\%$, $p = 0.036$) (Fig. 3). The AWTd of LAD ligated groups was decreased signif-

Table 1. Genes Upregulated in Bcl-2-Overexpressing L6 Myoblast Sheets Compared to Wild-Type Cell Sheets

Gene Name	Fold Change Up	Description
1372602_at	13.16	genethonin
1371126_x_at	8.017	granzyme B
1367782_at	7.712	cytochrome c oxidase, subunit VIa, polypeptide 2
1370694_at	6.571	tribbles homolog 3 (Drosophila)
1370464_at	6.491	ATP-binding cassette, subfamily B (MDR/TAP), member 1A
1369043_at	5.989	potassium voltage-gated channel, shaker-related subfamily, member 4
1397300_at	5.957	transcribed locus
1394681_at	5.947	aldo-keto reductase family 1, member C-like 1
1379402_at	5.815	ATP-binding cassette, subfamily C (CFTR/MRP), member 4
1386185_at	5.524	tripartite motif-containing 7
1368918_at	5.513	placental growth factor
1369772_at	5.027	solute carrier family 6 (neurotransmitter transporter, glycine), member 9
1373282_at	5.017	similar to mitochondrial carrier protein MGC4399
1389066_at	4.691	regulator of calcineurin 2
1369343_at	4.653	glutamate receptor interacting protein 1
1373807_at	2.244	vegf-A

Table 2. Echocardiography Data at 3, 10, and 28 Days After LAD Ligation and Transplantation

	AWTd	PWTd	Dd	AWTs	PWTs	Ds	FS	EF
3 days								
Sham ($n = 5$)	1.28 ± 0.08	1.28 ± 0.10	8.02 ± 0.24	1.82 ± 0.12	1.88 ± 0.12	6.00 ± 0.21	0.252 ± 0.013	0.580 ± 0.022
Control $n = 22$	1.18 ± 0.04	1.45 ± 0.04	8.18 ± 1.13	1.21 ± 0.04	2.11 ± 0.07	7.02 ± 0.11§	0.140 ± 0.012§	0.357 ± 0.024§
L6-WT ($n = 17$)	1.08 ± 0.06	1.45 ± 0.05	7.84 ± 0.18†	1.06 ± 0.06†§	1.99 ± 0.09	6.91 ± 0.14§	0.116 ± 0.010§	0.306 ± 0.022§
L6-Bcl2 ($n = 21$)	1.06 ± 0.05*†	1.39 ± 0.05	8.35 ± 0.13‡	1.08 ± 0.04†§	2.07 ± 0.07	7.34 ± 0.14*‡§	0.121 ± 0.010§	0.314 ± 0.023§
10 days								
Sham ($n = 5$)	1.38 ± 0.04	1.46 ± 0.10	7.74 ± 0.30	1.86 ± 0.09	1.98 ± 0.06	6.02 ± 0.20	0.221 ± 0.015	0.525 ± 0.029
Control ($n = 22$)	0.58 ± 0.03§	1.51 ± 0.06	9.58 ± 0.16§	0.58 ± 0.03§	2.12 ± 0.07	8.50 ± 0.17§	0.114 ± 0.008§	0.300 ± 0.019§
L6-WT ($n = 17$)	0.59 ± 0.04§	1.37 ± 0.05†	9.28 ± 0.18§	0.65 ± 0.05§	2.12 ± 0.08	8.19 ± 0.18§	0.114 ± 0.010§	0.322 ± 0.021§
L6-Bcl2 ($n = 21$)	0.61 ± 0.03§	1.44 ± 0.06	9.44 ± 0.17§	0.60 ± 0.03§	2.33 ± 0.08*†‡	8.08 ± 0.15†§	0.144 ± 0.010†‡§	0.378 ± 0.019†‡§
28 days								
Sham ($n = 5$)	1.42 ± 0.04	1.62 ± 0.12	7.70 ± 0.35	1.74 ± 0.10	2.18 ± 0.16	5.94 ± 0.43	0.233 ± 0.027	0.542 ± 0.045
Control ($n = 22$)	0.60 ± 0.03§	1.53 ± 0.05	10.46 ± 0.17§	0.61 ± 0.03§	2.16 ± 0.09	9.38 ± 0.22§	0.106 ± 0.008§	0.280 ± 0.020§
L6-WT ($n = 17$)	0.55 ± 0.04§	1.55 ± 0.07	10.11 ± 0.14§	0.52 ± 0.04†§	2.20 ± 0.07	9.04 ± 0.14§	0.106 ± 0.006§	0.285 ± 0.014§
L6-Bcl2 ($n = 21$)	0.63 ± 0.03‡§	1.75 ± 0.07†‡	10.61 ± 0.17§	0.64 ± 0.03‡§	2.48 ± 0.09†‡	9.27 ± 0.18§	0.127 ± 0.008†‡§	0.331 ± 0.019†‡§

Values represent mean ± SEM of anterior and posterior wall thickness in diastolic (AWTd, PWTd) and systolic phases (AWTs, PWTs) and left ventricular diameter in diastolic (Dd) and systolic (Ds) phases. Units are presented in mm. Dd and Ds were used to calculate fraction shortening (LVFS) and ejection fraction (LVEF) percentage.

*$p < 0.05$ compared to sham-operated group.

†$p < 0.05$ compared to control group.

‡$p < 0.05$ compared to L6-WT group.

§$p < 0.001$ compared to sham-operated group.

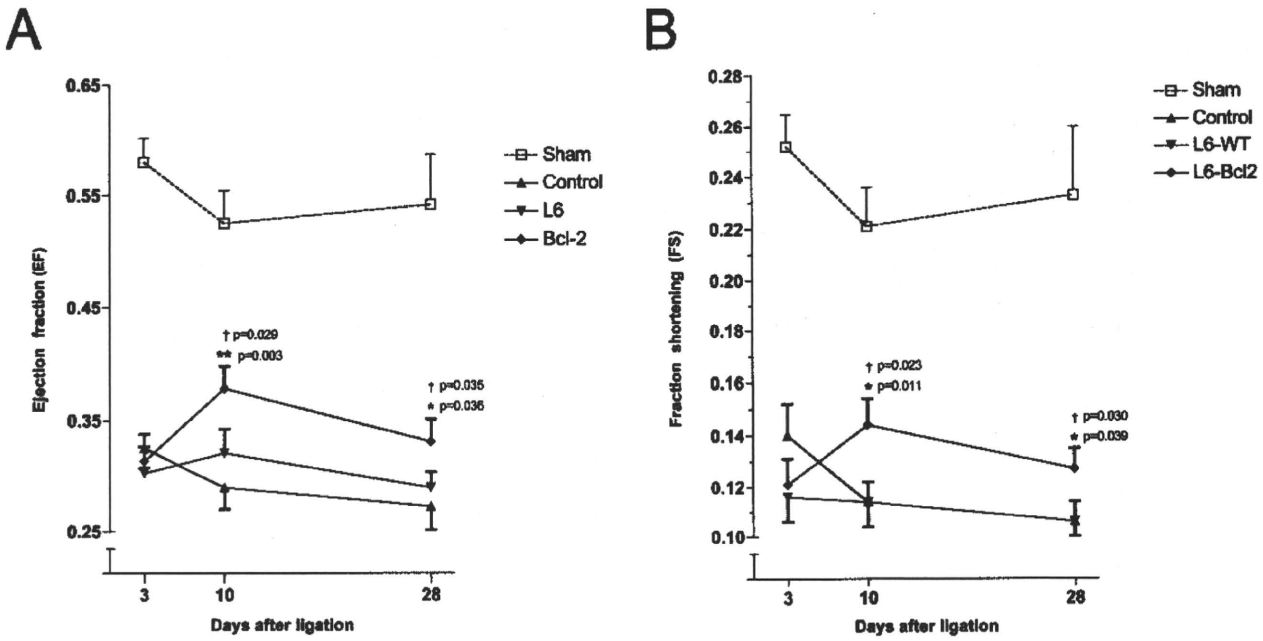

Figure 3. Echocardiography for (A) left ventricle ejection fraction (EF) and (B) left ventricle fraction shortening at the indicated time points after wild-type ($n = 17$, L6-WT) and Bcl-2-overexpressing ($n = 20$, L6-Bcl2) myoblast sheet therapy for acute myocardial infarction (AMI). Control rats ($n = 22$) underwent AMI without sheet transplantation, and sham-operated rats ($n = 5$) underwent left-sided thoracotomy to control the surgery-induced effect on systolic parameters. $*p < 0.05$, $**p < 0.01$ compared to the control group; $\dagger p < 0.05$, $\dagger\dagger p < 0.01$ compared to the L6-WT group.

icantly from baseline and was thinner than that of the sham group at day 10 ($p < 0.001$), and remained as such until day 28. PWTd was significantly higher in the L6-Bcl2 group than in the control and L6-WT groups at day 28.

Myoblast Sheets Expressing Bcl-2 Exert Therapeutic Effects on Injured Myocardium

Because Bcl-2 expression improved the myoblast sheet production of angiogenic growth factors, such as VEGF and PlGF, we evaluated the end-point vessel density after sheet transplantation. Higher vessel density was evident with vWF immunostaining at the infarct area on which the sheets were placed (Fig. 4). This area thus received maximal concentrations of growth factors and paracrine stimulation deriving from the sheets. Paracrine effects of myoblast sheet transplantation were also observed in the border area, and to a lesser extent, in the remote area, suggesting an enhanced effect of L6-Bcl2 sheets. The higher vascular density was associated with decreased fibrosis. The L6-Bcl2 group showed a significantly lower percentage of fibrosis than did the control and L6-WT groups (L6-Bcl2: $21.2 \pm 0.8\%$, vs. control: $25.6 \pm 1.8\%$, $p = 0.001$, and L6-WT: $24.6 \pm 1.6\%$, $p = 0.035$) (Fig. 5).

Cell death in AMI has been shown to occupy various forms ranging from overt necrosis to programmed apoptosis (27). To understand how myoblast sheet transplantation influences apoptosis and proliferation, we evaluated the expression of active caspase-3 as well as that of the proliferation-associated Ki67 antigen. No differences between groups in caspase-3-positive cells were found at the end of the study period (data not shown). In contrast, the number of proliferating cells within the myocardium was increased in groups receiving myoblast sheet transplantation (Fig. 6). In the L6-Bcl2 group, a significant number of proliferating cells was also found in the remote area (L6-Bcl2: 47.5 ± 3.7 vs. control: 30.9 ± 3.5, $p = 0.002$ or L6-WT: 31.9 ± 3.3, $p = 0.003$), further suggesting an increased paracrine effect. Because the higher number of proliferating cells, taken together with enhanced cardiac function, suggests activation of a regenerative response, we evaluated the amount of c-kit-positive cells in the myocardium. We found the number of cells positive for stem cell antigen c-kit to be significantly higher in the L6-Bcl2 group than in either the control group or the L6-WT group (L6-Bcl2: 52.3 ± 5.4 cells vs. control: 35.7 ± 6.1, $p = 0.029$ or L6-WT: 36.8 ± 5.4 cells, $p = 0.027$) (Fig. 7). All analyses of immunostainings were performed in a blinded fashion using computer-assisted automated evaluation.

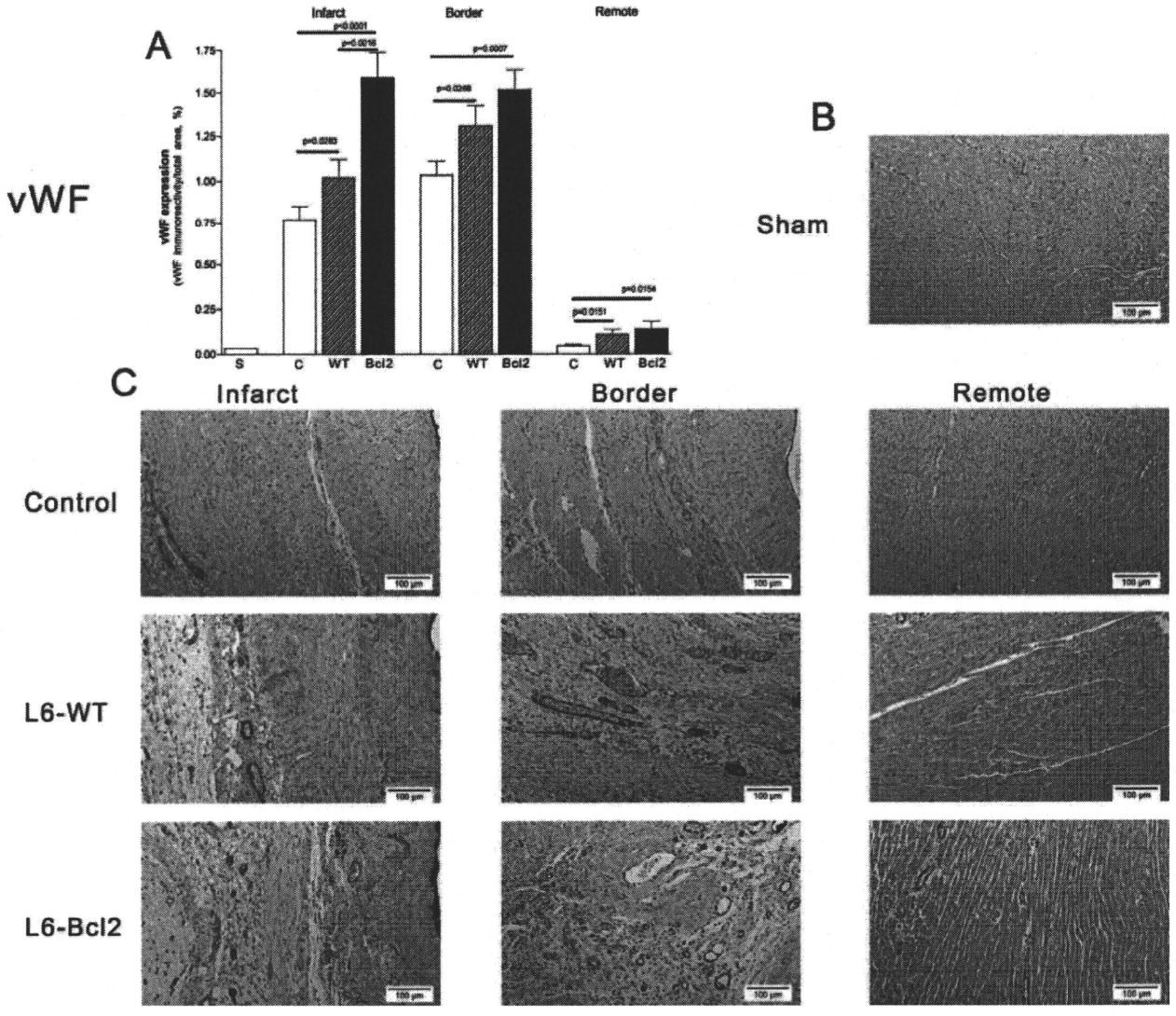

Figure 4. (A) Quantitative evaluation of vascular density using immunohistochemical staining for von Willebrand factor (vWF) expression in myocardial paraffin-embedded sections from sham-operated, wild-type (L6-WT), Bcl-2 (L6-Bcl2), and control animals. $*p < 0.05$, $**p < 0.01$ compared to the control group; $\dagger p < 0.05$, $\dagger\dagger p < 0.01$ compared to the L6-WT group. (B) Expression of vWF in uninfarcted, sham-operated myocardium. (C) Representative figures showing vascular density with vWF staining (dark staining) in infarct (left panels), border (middle panels), and remote (right panels) areas of the left ventricle. Sections were counterstained with hematoxylin.

Bcl-2 Enhances Myoblast Sheets Survival In Vivo

To demonstrate the enhanced survival of sheets by Bcl-2 expression in vivo, we generated GFP-expressing L6-WT or L6-Bcl2 myoblast sheets. These sheets were then transplanted onto the infarcted hearts as in previous experiments. We found that after 3 weeks, animals receiving L6-Bcl2 ($n = 6$) sheets showed 2.1-fold higher green fluorescence intensity in the heart than did the L6-WT ($n = 6$) group ($p = 0.006$) (Fig. 8A), suggesting that the Bcl-2-expressing myoblast sheets outlive their wild-type controls also in the harsh in vivo conditions (Fig. 8B). Furthermore, these data suggest that the myoblast sheets remain at the location of transplantation after surgery.

DISCUSSION

In AMI, the occlusion of a coronary artery blocks the oxygen and nutrient supply to the myocardium it supplied, and causes severe stress as well as cell death (16). Under these conditions, cell death occurs via several mechanisms ranging from programmed apoptosis to overt necrosis (27). The dying cells release mediators

that not only alert the immune system, but also promote cell death and exacerbate the damage (32). Moreover, reperfusion may further aggravate the rate of cell death (28). Prior studies have shown that Bcl-2 expression can protect cells transplanted for therapy by injection under these conditions (19). In this study, we investigated the ability of antiapoptotic Bcl-2 in myoblasts to functionally enhance cell sheet transplantation in a rat model of AMI. We show here that Bcl-2 expression can enhance the novel technique of myoblast sheet transplantation. Sheets expressing Bcl-2 had increased tolerance for apoptotic stimuli, and survived longer when transplanted on top of infarcted myocardium. Moreover, we show that introducing Bcl-2 expression in myoblast sheets lead to their enhanced production of proangiogenic mediators, specifically VEGF and PlGF. Therapy with Bcl-2-expressing myoblast sheets significantly improved cardiac function, reduced fibrosis, enhanced myocardial neoangiogenesis and cell proliferation, and increased the amount of the stem cell antigen, c-kit, positive cells in the myocardium.

Bcl-2 localizes intracellularly to mitochondrial, nuclear, and endoplasmic reticulum membranes (1). It protects cells from death stimuli, such as nutrient deprivation (36), by stabilizing the mitochondrial membrane potential (30), reducing caspase activation, or inhibiting cytochrome c release (9). While tissue regeneration therapies and cell transplantation therapy aim to replace dead cells with progenitors as well as introducing growth-promoting signals to the tissue environment (19), it is frequently forgotten that transplanted cells face the same severe surroundings. Although studies have demonstrated the superiority of cell sheet therapy to intramyocardial injections in heart failure (20), transplantation of several sheets is required to counteract the struggle for survival, nutrients, and oxygen.

Mechanisms of cell death operating under ischemia and infarction depend on the location of cells in relation

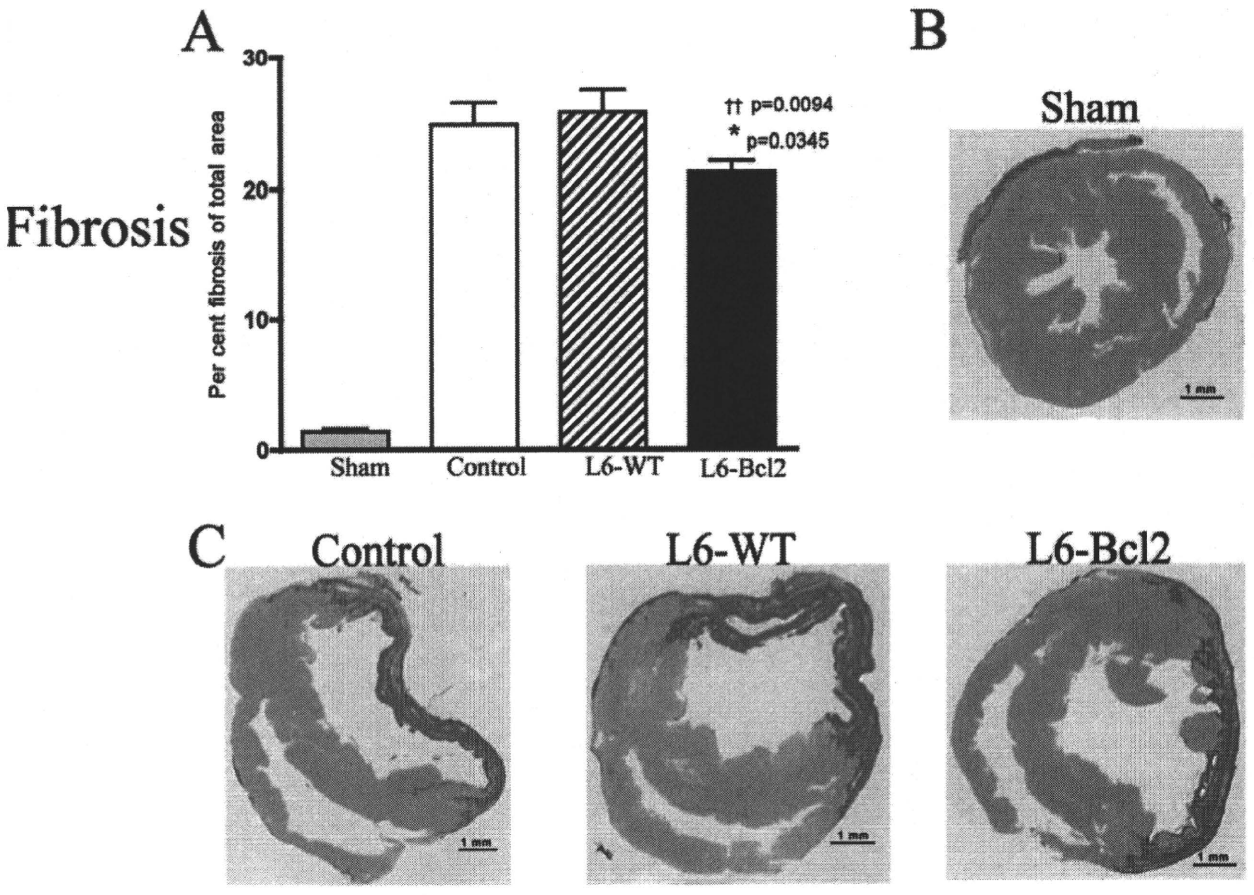

Figure 5. (A) Quantitative evaluation of fibrosis by Sirius Red staining of myocardial paraffin-embedded sections from sham-operated, wild-type (L6-WT), Bcl-2 (L6-Bcl2), and control animals. $*p < 0.05$, $**p < 0.01$ compared to the control group; $\dagger p < 0.05$, $\dagger\dagger p < 0.01$ compared to the L6-WT group. (B) Background staining in uninfarcted, sham-operated myocardium. (C) Representative figures showing the amount of fibrosis (darker gray shading) in infarct (left panels), border (middle panels), and remote (right panels) areas of the left ventricle.

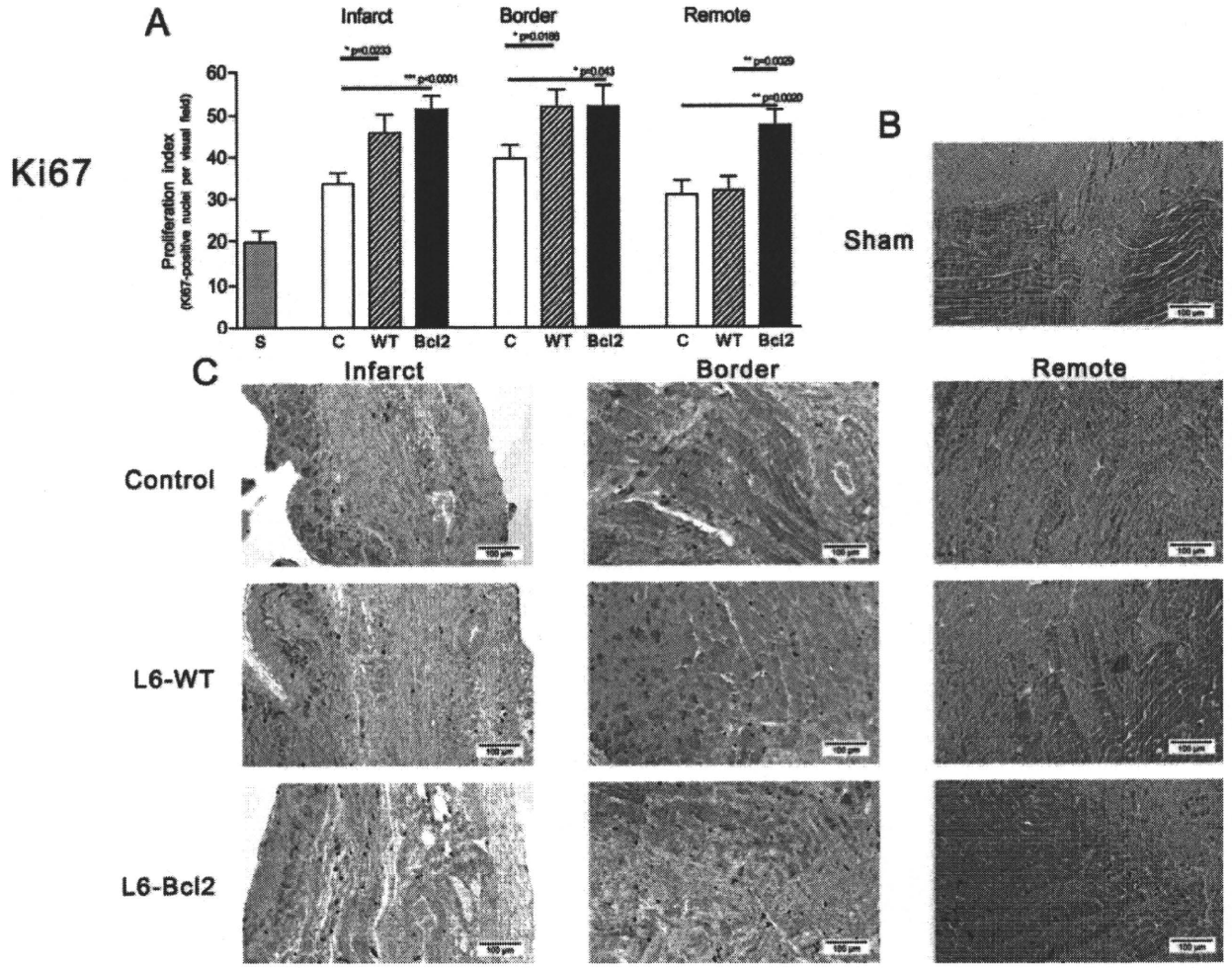

Figure 6. (A) Quantitative evaluation of proliferative cells as assessed with the expression of proliferation associated Ki67 nuclear antigen (dark brown). Figure shows mean ± SEM densitometry values from the immunohistochemistry of myocardial paraffin-embedded sections of sham-operated, wild-type (L6-WT), Bcl-2 (L6-Bcl2), and control animals. $*p < 0.05$, $**p < 0.01$ compared to the control group, $\dagger p < 0.05$, $\dagger\dagger p < 0.01$ compared to the L6-WT group. (B) Expression of Ki67 in uninfarcted, sham-operated myocardium. (C) Representative figures of showing proliferating cells by Ki67 expression in infarct (left panels), border (middle panels), and remote (right panels) areas of the left ventricle. Sections were double-stained to detect muscle tissue by tropomyosin (darker staining) expression. Sections were counterstained with hematoxylin.

to the area supplied by the stenosed or occluded artery. Overt necrosis is predominant in the core areas, with programmed death by apoptosis gaining more ground towards the border areas with some collateral blood flow. The restricted oxygen and nutrient supply, along with cell debris released by necrotic cells, elicits cell death responses that operate through common mechanisms, such as the generation of reactive oxygen species (16) and target mitochondrial function (26). In this study, we mimicked these in vivo conditions in cell culture by removing serum from the culture medium, thus depriving cells of nutrients and growth factors. Moreover, to reproduce the proapoptotic environment of the infarcted area, we treated cells with staurosporine, a widely used inducer of apoptosis that elicits similar intracellular apoptotic cascades that spur cell death in infarcted myocardium (10). Bcl-2 overexpression in cells and cell sheets provided protection and resistance against both nutrient deprivation and staurosporine-induced apoptosis. Importantly, when stressed with nutrient deprivation myoblast sheets expressing Bcl-2 differentiated into myotubes. This suggests that expression of antiapoptotic Bcl-2 does not prevent the myoblasts to exit the cell cycle, fuse, and differentiate.

These results show the benefit of *bcl2* gene transduction for cell sheet transplantation, and corroborate with previous data on Bcl-2 expression inhibiting the mitochondrial pathway of apoptosis (18) activated by various

stress factors including serum deprivation (2) and oxidative stress (7). Interestingly, previous studies have shown that Bcl-2 expression, when introduced in the heart, provides myocardial protection against ischemia (13), and further validates our approach. Thus, the introduction of *bcl2* as a controlled pretransplantation gene therapy can be considered beneficial for promoting the effects of cell sheets under ischemic or infarcted tissues in prevailing proapoptotic or nutrient-deprived environments.

The finding that Bcl-2 expression only influences gene expression in cell sheets suggests that Bcl-2 does not alter cell behavior under normal growth conditions, Bcl-2 activity specifically enhances apoptosis tolerance, and that formation of cell sheets may induce apoptotic stress to the cells. These results show that when applying cell sheet therapy, prevention of apoptotic death already at the initial steps of sheet formation is necessary for maximizing therapeutic efficacy. In the Bcl-2-express-

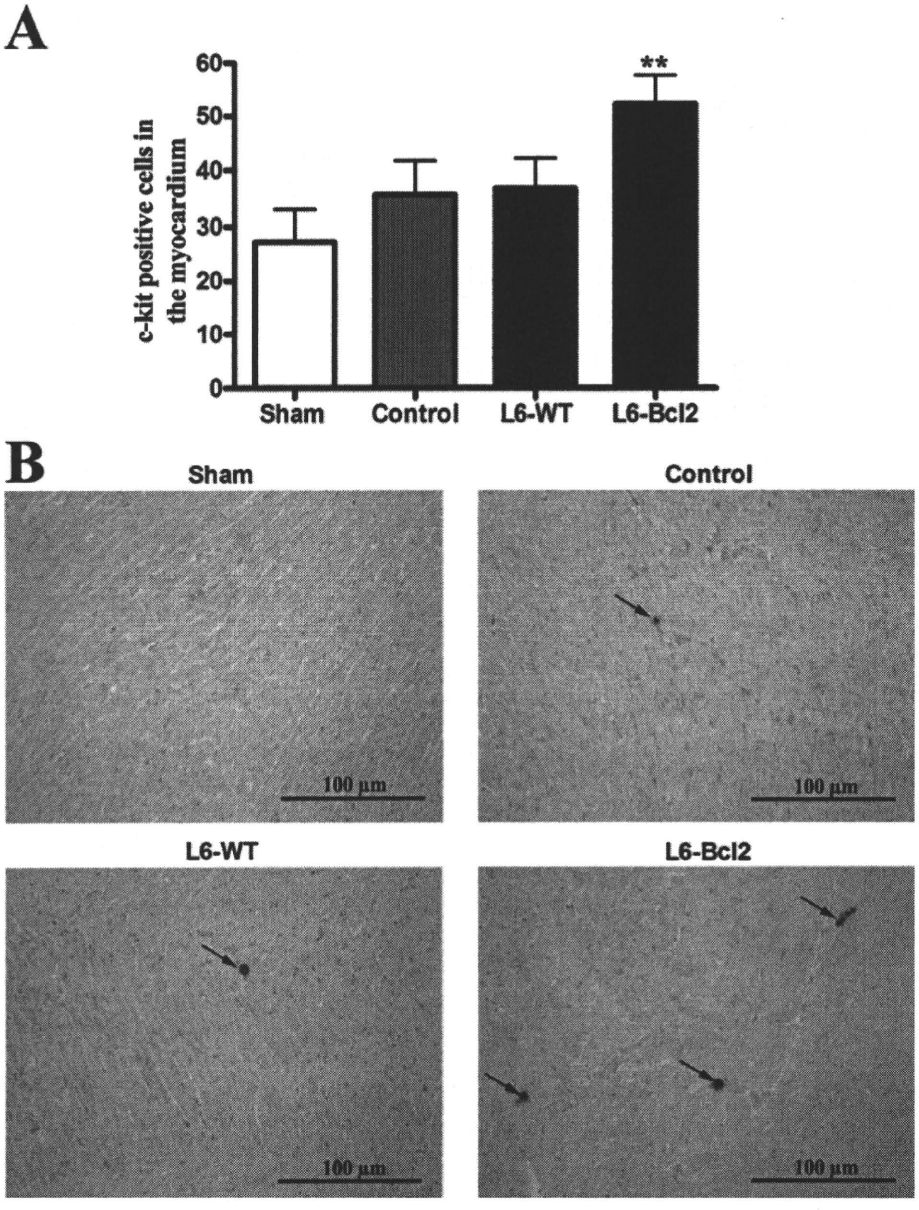

Figure 7. (A) Quantitative evaluation of the number of c-kit-expressing cells in the myocardium. Paraffin-embedded sections were stained from sham-operated, wild-type (L6-WT), Bcl-2 (L6-Bcl2), and control animals. $*p < 0.05$ compared to the L6-WT group, $**p < 0.01$ compared to the control group. (B) Representative figures of c-kit expressing cells in the myocardium from sham-operated (upper left panel), control (upper right panel), L6-WT (lower left panel), and L6-Bcl2 (lower right panel) groups. Sections were counterstained with Nuclear Fast Red.

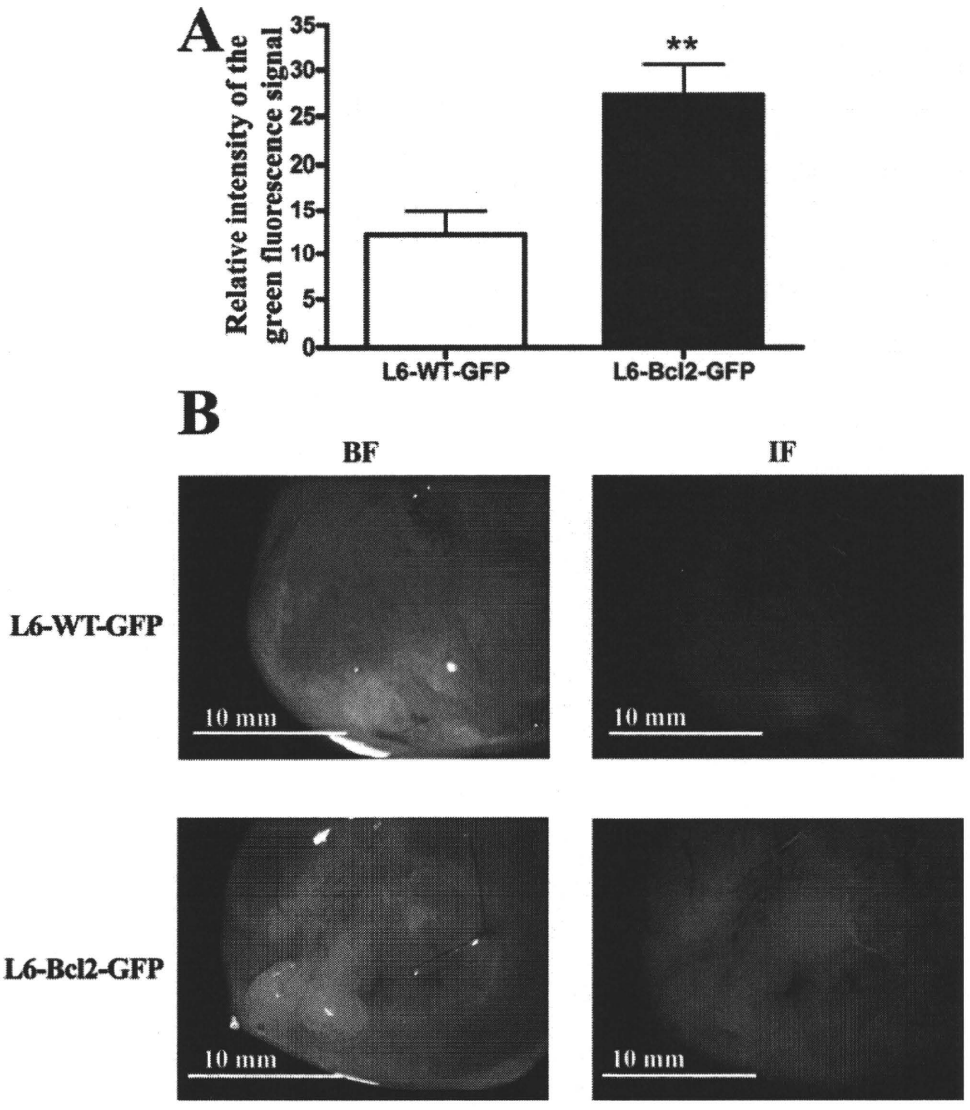

Figure 8. Quantitative evaluation of cell survival after myoblast cell sheet transplantation. (A) Analysis of green fluorescence intensity from the apical surface of hearts 3 weeks after transplantation of GFP-expressing wild-type (L6-WT-GFP, $n = 6$) and Bcl-2-overexpressing (L6-Bcl2-GFP, $n = 6$) cell sheets. (B) Representative bright field (left panels) or fluorescence (right panels) images of excised hearts three weeks after surgery.

ing myoblast sheets we observed enhanced production of the VEGF family paracrine effectors, VEGF-A and PlGF. These growth factors are known to synergize in proangiogenic signaling (24), and further add to the beneficial profile induced by introduction of Bcl-2. In a previous study, Memon and colleagues reported that the myocardium under the myoblast sheets produces growth factors, such as VEGF (20). In this study, we show that wild-type myoblast sheets themselves exhibit enhanced production of proangiogenic factors compared to standard cultures of myoblasts, and that expression of Bcl-2 in sheets greatly enhances the production of these paracrine factors.

To further test the Bcl-2-mediated functional therapeutic benefit in vivo in AMI, wild-type, and Bcl-2-expressing sheets were transplanted onto the ischemic myocardium after LAD ligation. In the group undergoing Bcl-2 sheet transplantation, clearly enhanced left ventricular function was already evident at 10 days and was sustained until the end of the study period, 28 days after transplantation. LVEF paralleled LVFS as an alternate measure for left ventricular performance. Although

some studies have reported enhanced cardiac function by unmodified myoblast sheets in experimental models of MI (11,20), treatment with two layers of wild-type sheets in this study did not significantly increase LVEF. Here, however, transplantation of wild-type sheets also counteracted the LVEF decline after MI. This may be due to differences in rat strain (20), host species of donor myoblasts (11), the low number of cell sheets used, or the acute infarction model employed in the current study. Furthermore, due to generation and passage of the L6 cell line, differences to primary cells, as used in some studies, may emerge (35). Sheet transplantation increased vascular density in infarcted and border areas as evaluated by vWF immunostaining. Only the Bcl-2-modified sheet therapy increased both the number of proliferating cells in the remote area and the number of cells positive for stem cell antigen c-kit in the myocardium. In view of a recent report by Cimini et al. (8), these results suggest that more stem cells are stimulated to infiltrate the myocardium by Bcl-2-modified myoblast sheet therapy. Induction of stem cell infiltration can subsequently activate the endogenous repair processes of the myocardium (8). The observed effects on angiogenesis, proliferation, and c-kit expression were associated with an antifibrotic effect of the sheets at 28 days. Furthermore, overexpression of Bcl-2 resulted in prolonged survival of myoblast sheets in vivo, providing sustained secretion of angiogenic factors. The importance of such paracrine activators from myoblasts was demonstrated by Perez-Ilzarbe and colleagues on endothelial, smooth muscle, and cardiomyocyte cells (25). Activation of all these cell types is required for efficient repair of the damaged myocardium.

Taken together these results suggest that Bcl-2 overexpression in the myoblast sheets enhances their therapeutic potential by improving and sustaining the paracrine effects of the sheets in AMI. To our knowledge, this study presents the first combination therapy approach to use gene therapy-engineered cell sheets that can withstand apoptosis induction by means of Bcl-2 expression. These results provide the first insight on how antiapoptotic and mitochondrioprotective strategies not only functionally but also by specific modification of gene expression profile can enhance the novel approach of cell sheet transplantation therapy in treatment of heart failure. Because myoblast sheet transplantation has shown no adverse effects in either preclinical or clinical settings (Y. Sawa, personal communication), it seems feasible to adopt this cell transplantation methodology for gene modification and as vehicle in gene therapy as well. The transplantation of sheets can easily be carried out in conjunction with coronary artery bypass surgery, and it produces minimal damage to the heart muscle compared to cell injections. The cells can be transduced with an optimized minimal amount of viral vector, and no viral vectors are injected to the patient. However, clinical trials are warranted to unambiguously demonstrate the efficacy of cell sheet transplantation.

ACKNOWLEDGMENTS: This project was supported by Academy of Finland, Finnish Funding Agency of Technology and Innovation, Japanese Society for the Promotion of Science, and Japan Science and Technology Agency. We thank Lahja Eurajoki for her help with the cell cultures and measurements, Irina Suomalainen for the immunohistochemical staining, and Anne Reijula for the tissue processing. We also thank Veikko Huusko, Virpi Norppo, Kari Savelius, and Olli Valtanen for all their help and for the excellent animal care.

REFERENCES

1. Adams, J. M.; Cory, S. The Bcl-2 protein family: Arbiters of cell survival. Science 281:1322–1326; 1998.
2. Bialik, S.; Cryns, V. L.; Drincic, A.; Miyata, S.; Wollowick, A. L.; Srinivasan, A.; Kitsis, R. N. The mitochondrial apoptotic pathway is activated by serum and glucose deprivation in cardiac myocytes. Circ. Res. 85:403–414; 1999.
3. Bizik, J.; Kankuri, E.; Ristimaki, A.; Taieb, A.; Vapaatalo, H.; Lubitz, W.; Vaheri, A. Cell–cell contacts trigger programmed necrosis and induce cyclooxygenase-2 expression. Cell Death Differ. 11:183–195; 2004.
4. Bouju, S.; Lignon, M. F.; Pietu, G.; Le Cunff, M.; Leger, J. J.; Auffray, C.; Dechesne, C. A. Molecular cloning and functional expression of a novel human gene encoding two 41–43 kDa skeletal muscle internal membrane proteins. Biochem. J. 335:549–556; 1998.
5. Chao, D. T.; Korsmeyer, S. J. BCL-2 family: Regulators of cell death. Annu. Rev. Immunol. 16:395–419; 1998.
6. Chinnaiyan, A. M.; Orth, K.; O'Rourke, K.; Duan, H.; Poirier, G. G.; Dixit, V. M. Molecular ordering of the cell death pathway. Bcl-2 and Bcl-xL function upstream of the CED-3-like apoptotic proteases. J. Biol. Chem. 271:4573–4576; 1996.
7. Choi, H.; Kim, S. H.; Chun, Y. S.; Cho, Y. S.; Park, J. W.; Kim, M. S. In vivo hyperoxic preconditioning prevents myocardial infarction by expressing bcl-2. Exp. Biol. Med. (Maywood) 231:463–472; 2006.
8. Cimini, M.; Fazel, S.; Zhuo, S.; Xaymardan, M.; Fujii, H.; Weisel, R. D.; Li, R. K. C-Kit dysfunction impairs myocardial healing after infarction. Circulation 116:I77–82; 2007.
9. Crow, M. T.; Mani, K.; Nam, Y. J.; Kitsis, R. N. The mitochondrial death pathway and cardiac myocyte apoptosis. Circ. Res. 95:957–970; 2004.
10. Gil, J.; Almeida, S.; Oliveira, C. R.; Rego, A. C. Cytosolic and mitochondrial ROS in staurosporine-induced retinal cell apoptosis. Free Radic. Biol. Med. 35:1500–1514; 2003.
11. Hamdi, H.; Furuta, A.; Bellamy, V.; Bel, A.; Puymirat, E.; Peyrard, S.; Agbulut, O.; Menasche, P. Cell delivery: Intramyocardial injections or epicardial deposition? A head-to-head comparison. Ann. Thorac. Surg. 87:1196–1203; 2009.
12. Hata, H.; Matsumiya, G.; Miyagawa, S.; Kondoh, H.; Kawaguchi, N.; Matsuura, N.; Shimizu, T.; Okano, T.; Matsuda, H.; Sawa, Y. Grafted skeletal myoblast sheets

attenuate myocardial remodeling in pacing-induced canine heart failure model. J. Thorac. Cardiovasc. Surg. 132: 918–924; 2006.
13. Imahashi, K.; Schneider, M. D.; Steenbergen, C.; Murphy, E. Transgenic expression of Bcl-2 modulates energy metabolism, prevents cytosolic acidification during ischemia, and reduces ischemia/reperfusion injury. Circ. Res. 95: 734–741; 2004.
14. Klefstrom, J.; Vastrik, I.; Saksela, E.; Valle, J.; Eilers, M.; Alitalo, K. c-Myc induces cellular susceptibility to the cytotoxic action of TNF-alpha. EMBO J. 13:5442–5450; 1994.
15. Kondoh, H.; Sawa, Y.; Miyagawa, S.; Sakakida-Kitagawa, S.; Memon, I. A.; Kawaguchi, N.; Matsuura, N.; Shimizu, T.; Okano, T.; Matsuda, H. Longer preservation of cardiac performance by sheet-shaped myoblast implantation in dilated cardiomyopathic hamsters. Cardiovasc. Res. 69: 466–475; 2006.
16. Krijnen, P. A.; Nijmeijer, R.; Meijer, C. J.; Visser, C. A.; Hack, C. E.; Niessen, H. W. Apoptosis in myocardial ischaemia and infarction. J. Clin. Pathol. 55:801–811; 2002.
17. Kutschka, I.; Kofidis, T.; Chen, I. Y.; von Degenfeld, G.; Zwierzchoniewska, M.; Hoyt, G.; Arai, T.; Lebl, D. R.; Hendry, S. L.; Sheikh, A. Y.; Cooke, D. T.; Connolly, A.; Blau, H. M.; Gambhir, S. S.; Robbins, R. C. Adenoviral human BCL-2 transgene expression attenuates early donor cell death after cardiomyoblast transplantation into ischemic rat hearts. Circulation 114:I174–180; 2006.
18. Kuwana, T.; Newmeyer, D. D. Bcl-2-family proteins and the role of mitochondria in apoptosis. Curr. Opin. Cell Biol. 15:691–699; 2003.
19. Li, W.; Ma, N.; Ong, L. L.; Nesselmann, C.; Klopsch, C.; Ladilov, Y.; Furlani, D.; Piechaczek, C.; Moebius, J. M.; Lutzow, K.; Lendlein, A.; Stamm, C.; Li, R. K.; Steinhoff, G. Bcl-2 engineered MSCs inhibited apoptosis and improved heart function. Stem Cells 25:2118–2127; 2007.
20. Memon, I. A.; Sawa, Y.; Fukushima, N.; Matsumiya, G.; Miyagawa, S.; Taketani, S.; Sakakida, S. K.; Kondoh, H.; Aleshin, A. N.; Shimizu, T.; Okano, T.; Matsuda, H. Repair of impaired myocardium by means of implantation of engineered autologous myoblast sheets. J. Thorac. Cardiovasc. Surg. 130:1333–1341; 2005.
21. Naro, F.; Sette, C.; Vicini, E.; De Arcangelis, V.; Grange, M.; Conti, M.; Lagarde, M.; Molinaro, M.; Adamo, S.; Nemoz, G. Involvement of type 4 cAMP-phosphodiesterase in the myogenic differentiation of L6 cells. Mol. Biol. Cell 10:4355–4367; 1999.
22. Okano, T.; Yamada, N.; Okuhara, M.; Sakai, H.; Sakurai, Y. Mechanism of cell detachment from temperature-modulated, hydrophilic-hydrophobic polymer surfaces. Biomaterials 16:297–303; 1995.
23. Palojoki, E.; Saraste, A.; Eriksson, A.; Pulkki, K.; Kallajoki, M.; Voipio-Pulkki, L. M.; Tikkanen, I. Cardiomyocyte apoptosis and ventricular remodeling after myocardial infarction in rats. Am. J. Physiol. Heart Circ. Physiol. 280:H2726–2731; 2001.
24. Payne, T. R.; Oshima, H.; Okada, M.; Momoi, N.; Tobita, K.; Keller, B. B.; Peng, H.; Huard, J. A relationship between vascular endothelial growth factor, angiogenesis, and cardiac repair after muscle stem cell transplantation into ischemic hearts. J. Am. Coll. Cardiol. 50:1677–1684; 2007.
25. Perez-Ilzarbe, M.; Agbulut, O.; Pelacho, B.; Ciorba, C.; San Jose-Eneriz, E.; Desnos, M.; Hagege, A. A.; Aranda, P.; Andreu, E. J.; Menasche, P.; Prosper, F. Characterization of the paracrine effects of human skeletal myoblasts transplanted in infarcted myocardium. Eur. J. Heart Fail. 10:1065–1072; 2008.
26. Regula, K. M.; Ens, K.; Kirshenbaum, L. A. Mitochondria-assisted cell suicide: A license to kill. J. Mol. Cell. Cardiol. 35:559–567; 2003.
27. Saraste, A.; Pulkki, K.; Kallajoki, M.; Henriksen, K.; Parvinen, M.; Voipio-Pulkki, L. M. Apoptosis in human acute myocardial infarction. Circulation 95:320–323; 1997.
28. Scarabelli, T. M.; Gottlieb, R. A. Functional and clinical repercussions of myocyte apoptosis in the multifaceted damage by ischemia/reperfusion injury: old and new concepts after 10 years of contributions. Cell Death Differ. 11(Suppl. 2):S144–152; 2004.
29. Seidel, M.; Borczynska, A.; Rozwadowska, N.; Kurpisz, M. Cell-based therapy for heart failure: Skeletal myoblasts. Cell Transplant. 18:695–707; 2009.
30. Shimizu, S.; Konishi, A.; Kodama, T.; Tsujimoto, Y. BH4 domain of antiapoptotic Bcl-2 family members closes voltage-dependent anion channel and inhibits apoptotic mitochondrial changes and cell death. Proc. Natl. Acad. Sci. USA 97:3100–3105; 2000.
31. Shimizu, T.; Yamato, M.; Isoi, Y.; Akutsu, T.; Setomaru, T.; Abe, K.; Kikuchi, A.; Umezu, M.; Okano, T. Fabrication of pulsatile cardiac tissue grafts using a novel 3-dimensional cell sheet manipulation technique and temperature-responsive cell culture surfaces. Circ. Res. 90: e40; 2002.
32. Umansky, S. R.; Tomei, L. D. Apoptosis in the heart. Adv. Pharmacol. 41:383–407; 1997.
33. Vaananen, A. J.; Salmenpera, P.; Hukkanen, M.; Rauhala, P.; Kankuri, E. Cathepsin B is a differentiation-resistant target for nitroxyl (HNO) in THP-1 monocyte/macrophages. Free Radic. Biol. Med. 41:120–131; 2006.
34. Vento, A.; Hammainen, P.; Patila, T.; Kankuri, E.; Harjula, A. Somatic stem cell transplantation for the failing heart. Scand. J. Surg. 96:131–139; 2007.
35. Yaffe, D. Retention of differentiation potentialities during prolonged cultivation of myogenic cells. Proc. Natl. Acad. Sci. USA 61:477–483; 1968.
36. Zhu, W.; Cowie, A.; Wasfy, G. W.; Penn, L. Z.; Leber, B.; Andrews, D. W. Bcl-2 mutants with restricted subcellular location reveal spatially distinct pathways for apoptosis in different cell types. EMBO J. 15:4130–4141; 1996.